Order Number 9304698

# Thermodynamics of linear defects in rocks and its application to an earthquake rebound theory

Majewski, Eugeniusz, Ph.D.

City University of New York, 1992

U·M·I
300 N. Zeeb Rd.
Ann Arbor, MI 48106

# THERMODYNAMICS OF LINEAR DEFECTS IN ROCKS AND ITS APPLICATION TO AN EARTHQUAKE REBOUND THEORY

by

EUGENIUSZ MAJEWSKI

A dissertation submitted to the Graduate Faculty in Earth and Environmental Sciences in partial fulfillment of the requirements for the degree of Doctor of Philosophy, The City University of New York

1992

This manuscript has been read and accepted for the Graduate Faculty in Earth and Environmental Sciences in satisfaction of the dissertation requirements for the degree of Doctor of Philosophy.

July 21, 1992
Date

Surendra K. Saxena
Chair of Examining Committee

July 21, 1992
Date

Daniel Habib
Executive Officer

Kathleen Crane

Somdev Bhattacharji

Supervisory Committee

THE CITY UNIVERSITY OF NEW YORK

Abstract

THERMODYNAMICS OF LINEAR DEFECTS IN ROCKS AND ITS APPLICATION TO AN EARTHQUAKE REBOUND THEORY

by

Eugeniusz Majewski

Adviser: Professor Surendra K. Saxena

The thesis deals with thermodynamics of linear defects (dislocations, linear vacancies and cracks) and its application to an earthquake rebound theory. A computer simulation of an earthquake is developed here. Theoretical results for the strain and stress, a seismic moment, and an entropy jump during an earthquake process are derived and compared with measurements of real earthquakes. An identification of material parameters was done by the Monte Carlo Method.

# PREFACE

The purpose of this thesis is to determine some constraints on mineralogical composition of the Earth's mantle. We formulate here a new theory of thermodynamics of linear defects in rocks and apply it to an earthquake rebound theory (Teisseyre, 1980, 1985a,b, 1987). Further, we deliver a computer simulation of an earthquake. From this simulation we compute an earthquake magnitude, stress and strain diagram as a function of time, a seismic moment, jump of entropy as a function of time during an earthquake, stress evolution and rebound motion in the framework of a new earthquake rebound theory which is further developed here. A difference between values of thermodynamical functions and constants derived from the aforementioned theory and respective values of the same functions and constants obtained from seismological measurements are treated here as aim functions. By an application of the Monte Carlo Method we seek a global minimum of an aim function. A local minimum can be found using the Gauss-Seidl Method. A set of parameters which gives the minimum will be treated as the most probable mineral composition of the earthquake focal zone. A model adoped in

in this paper assumes that a rock medium is permeated with a continuum field of linear defects and that a flow of defects describes an advanced state of deformation leading to fracturing and an earthquake. At the beginning a thermodynamical model of rock deformation and fracture is developed. Thermodynamics of linear defects like dislocations and cracks are formulated. Defect parameters are connected with bulk properties of a rock. The Gibbs defect energy is related to the shear bulk modulus of the rock. In this model the formation (as well as the migration and the activation) Gibbs energy for the linear defect is proportional to the bulk shear modulus and the lattice constant of rock-forming phases. A coefficient which is practically temperature and pressure independent and is fixed only by the defect mechanism and the matrix material (i.e., the mineral composition of the rock), is applied. An equation for a crack density which is a function of a dislocation density and the Gibbs defect energy, is developed. An additive decomposition of the crack density rate is assumed. Components of the crack density rate are responsible for the formation, growth, propagation and coalescence of cracks, and rock fracture, respectively. The crack density is employed in the evolution equation for a shear stress. This equation is applied to a numerical simulation of an earthquake sequence based on the rebound theory. A zone of earthquake development is modelled by a

a medium filled with linear defects. The energy release and stress drop are estimated as two main parameters of earthquake event. The agreement of the estimated values from this theory and the corresponding values obtained from measurements of different earthquakes at different depths, is discussed.

Acknowledgements

I am very grateful to Professor Surendra K. Saxena of the City University of New York and Uppsala University for his constant inspiration and helpful discussions during preparation of this paper.

I wish to thank Professor Kathy Crane of Hunter College and Lamont - Doherty Geological Observatory of the Columbia University and Professor S. Bhattacharji of the City University of New York for reviewing this thesis.

TABLE OF CONTENTS

# LISTS OF FIGURES

# PART 1

# REVIEW OF PREVIOUS WORK

## 1. Introduction

### 1.1. Thermodynamics of line defects

There is an extensive literature on the thermodynamics of point defects and their relation with bulk properties (e.g., the monograph by P.A. Varotsos and K.D. Alexopoulos, 1986). That branch of thermodynamics has also served as a basis for analyses of glide motions of dislocations, where the dislocations are regarded as line defects. This paper is an attempt to bring together a number of results, from both thermodynamics of point defects and thermodynamics of line defects, which can be used directly in solid Earth physics. We should emphasize that the thermodynamics of point defects is a somewhat more mature area than the thermodynamics of line defects. There are many difficulties involved in application of thermodynamics in describing dislocations. The literature on this subject is very limited; the attempts to solve the problem involved are very recent. Our present state of knowledge of the thermodynamics of dislocations is such that dislocations cannot exist as thermodynamically stable lattice

defects, as the Gibbs free energy has no minimum corresponding to any equilibrium concentration of dislocations. A crystal can always reduce its Gibbs free energy by reducing the number of dislocations it contains. This reduction is a basis of processes such as recovery of recrystallization, which enhance the ductility of crystals. In addition, every theoretical approach uses a line tension approximation. We know that departures from this assumption may occur, e.g., due to the attraction between neighbouring branches of a dislocation on either side of a discrete obstacle. The self-stresses decrease the glide resistance from that obtained from a line tension model. Thus, thermodynamics of dislocation involves distinct inconsistency. In order to account for it, the conception of the so-called superlattice is introduced.

## 1.2. Experimental evidence of dislocations in minerals

Dislocations have been observed directly in a wide variety of crystalline materials, including most important rock-forming minerals. Dislocations were first observed by etching cleaved crystals. If a newly cleaved surface is etched in the proper way, the material dissolves somewhat more readily where a dislocation line intersects the cleavage face, thereby forming an etch pit. The material around the dislocation is more soluble because the crystal structure is distorted. The three-dimensional shape of the dislocation line may be mapped out by continuing to dissolve away the crystal in a succession of grindings and etchings. Dislocations can also be viewed under a petrographic microscope in a translucent crystal if an opaque material precipitates along the dislocation line; for example, substitutional-impurity and interstitial atoms may diffuse into the dislocation, thereby "decorating" it. There are a number of experimental techniques for decorating dislocations, and occasionally dislocations are naturally decorated. Olivine, the main constituent of the upper mantle, may be decorated by heating in air at 900 Celsius degrees for an hour or so.

Dislocations can be observed with a number of techniques, such as decoration methods with precipitate particles (cf. Hull, 1975; Ranalli, 1987 for details), TEM (transmission electron

microscopy), X-ray diffraction, and field ion microscopy. The most commonly used technique is TEM, which relies on the scattering of electrons in the strained region around a dislocation; its resolution is of the order of 0.4 mm.

Large numbers of dislocations are present in all natural materials. The dislocation density is defined as the total length of dislocation lines per unit volume or, equivalently, the number of dislocations per unit area. Dislocations densities are usually very high, ranging from $10^{10}m^{-2}$ in well-annealed crystals
to $10^{15}m^{-2}$ or more in crystals that have undergone large plastic deformation. Dislocations are present even in the absence of external stress, as they can be built up within the crystal during its growth from a melt or can be nucleated at internal stress concentration centers such as second-phase particles and grain boundary triple points.

In Fig. 1.1. we present the optical photomicrograph of decorated dislocations in olivine. The orthogonal geometry of the dislocation lines reflects a strong crystallographic control on dislocation geometry, which is common in olivine (Suppe, 1989).

Fig. 1.1. Optical photomicrograph of decorated dislocations in olivine. The orthogonal geometry of the dislocation lines reflects a strong crystallographic control on dislocation geometry, which is common in olivine (Suppe, 1989).

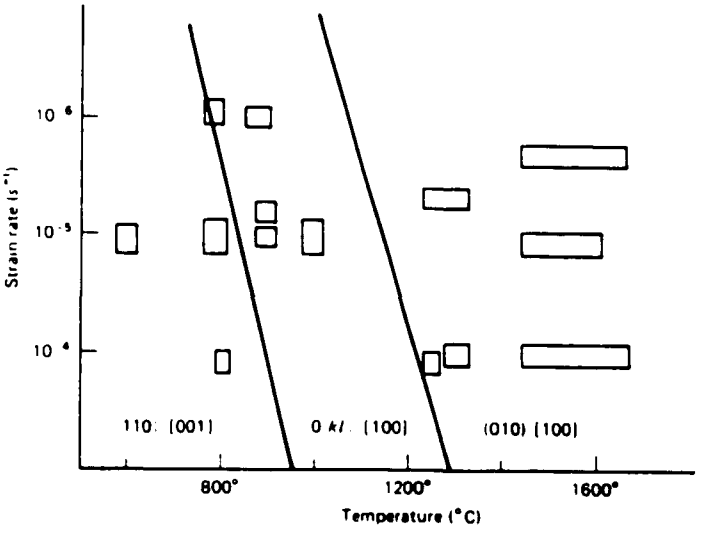


Fig. 1.2. Illustration of the dependence of the dominant slip system in olivine on experimental conditions of temperature and strain rate. Boxes represent experimental conditions. (Simplified from Carter and Ave'Lallement, Geol. Soc. Amer. Bull., v. 81, p. 2181-2202, 1970 by Suppe, 1989).

In Fig. 1.2. we show the illustration of the dependence of the dominant slip system in olivine on experimental conditions of temperature and strain rate. Boxes represent experimental conditions. This diagram was simplified from Carter and Ave'Lallement, Geol. Soc. Amer. Bull., v.81, p.2181-2202, 1970 by Suppe (1989).

In Fig. 1.3. we present the transmission electron micrographs of dislocations. The end points of the dislocations lie at the edge of the plane of focus in the crystal. (a) Nearly parallel set of dislocations in plagioclase feldspar. Dislocation density is 5.0 x $10^8 cm^{-2}$. Naturally deformed quartzo-feldspathic gneiss near Prince Rupert, British Columbia. (b) Free dislocations in quartz. Dislocation density 4.3 x $10^8 cm^{-2}$. Permian Verrucano Formation, low greenschist facies, Switzerland. (c) Tangled dislocations in quartz. Dislocation density 2.6 x $10^8 cm^{-2}$. Triassic Mels Quartzite, Switzerland. (d) Free dislocations and two walls of dislocations in Mels Quartzite. (Micrographs courtesy of B. Douglas and L. Pringle, from Suppe, 1989).

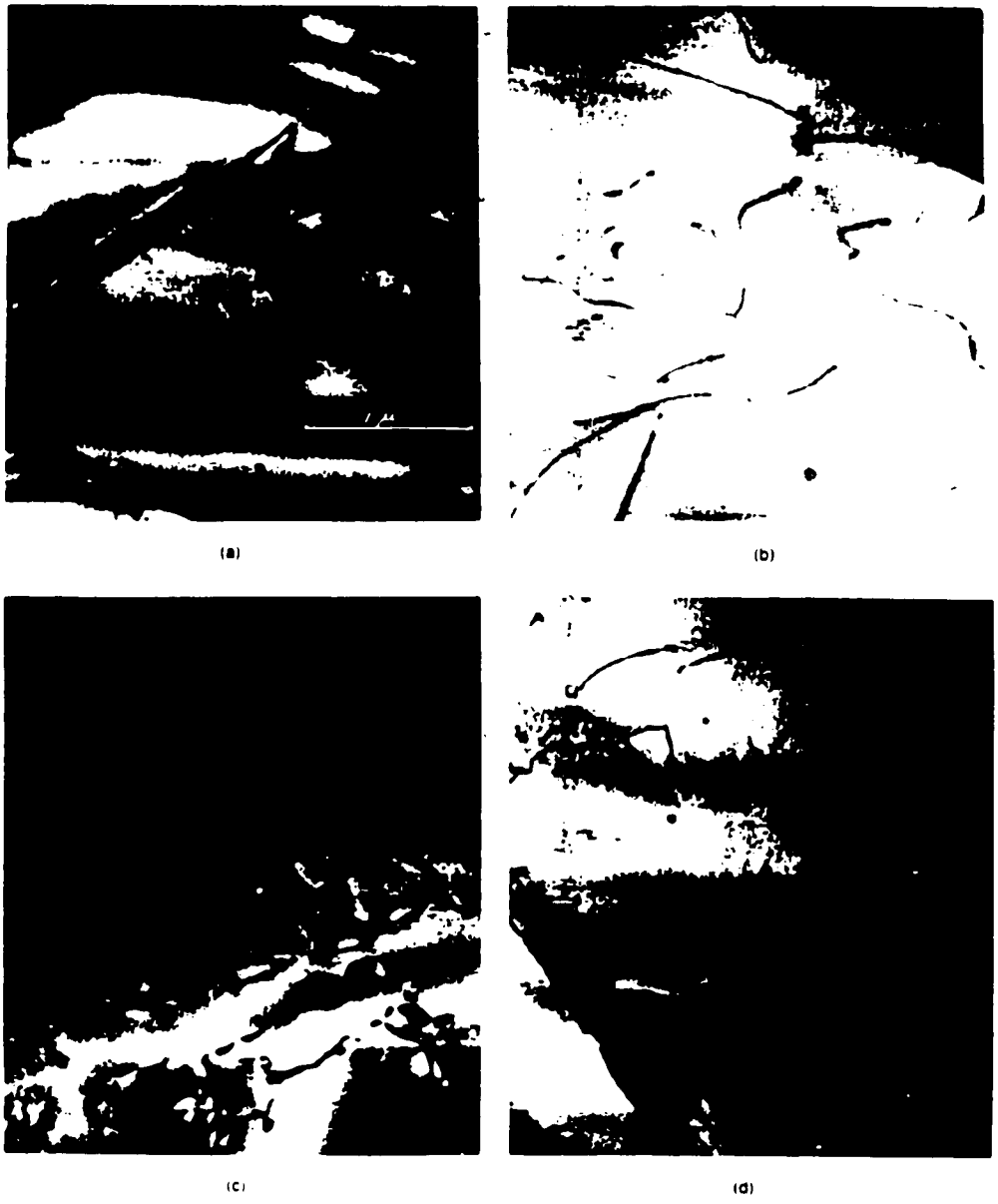


Fig. 1.3. Transmission electron micrographs of dislocations. The end points of the dislocations lie at the edge of the plane of focus in the crystal. (a) Nearly parallel set of dislocations in plagioclase feldspar. Dislocation density is $5.0 \times 10^{8} cm^{-2}$. (b) Free dislocations in quartz. Dislocation density $4.3 \times 10^{8} cm^{-2}$. (c) Tangled dislocations in quartz. Dislocation density $2.6 \times 10^{8} cm^{-2}$. (d) Free dislocations and two walls of dislocations in Mels Quartzite. (Micrographs courtesy of B. Douglas and L. Pringle. See Suppe, 1989).

## 1.3. Experimental tests on the rock strength

In this section we review two experimental tests on the rock strength. In Fig. 1.4. we can observe the compression stress-strain curves for shale from experiments by Peng and Podniesk (1972). Each curve corresponds to a different strain rate. In Fig. 1.5. we can see the compression stress-strain curves for sandstone from experiments with different strain rates by Bieniawski (1970).

After review of these results and of some other experimental stress-strain curves it is concluded that both the rupture stress and the corresponding strain are rate dependent. Although some differences in quantitative results occurred in various tests, a common qualitative conclusion could be drawn, namely: when the rate of straining or stressing increases, then both the rupture (or fracture) stress and the initial Young modulus of elasticity of the tested rock increase as well. In this paper some experimental and theoretical aspects of rock fracture on a macroscopic and microscopic level will be discussed in great detail.

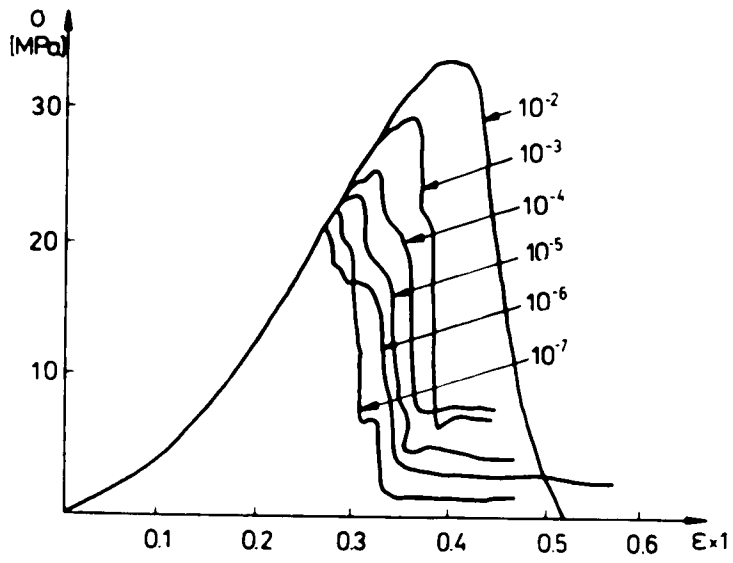


Fig. 1.4. Compression stress - strain curves for shale from experiments by Peng and Podniesk (1972). Each curve corresponds to different strain rate.

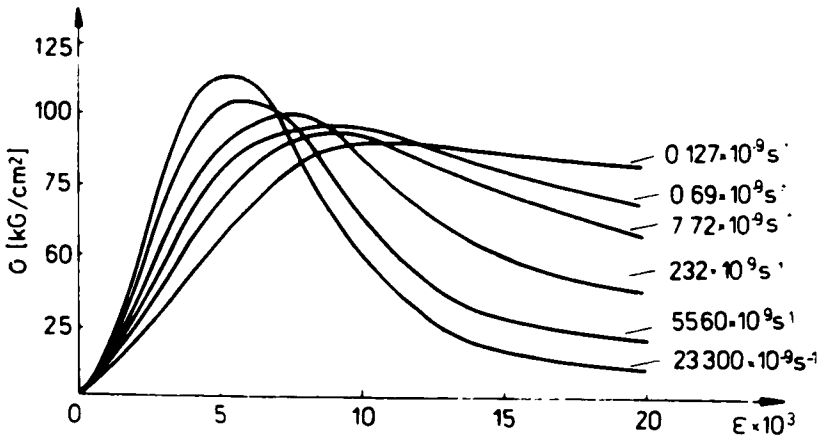


Fig. 1.5. Compression stress - strain curves for sandstone from experiments with different strain rates (Bieniawski, 1970).

## 1.4. The subduction of the lithosphere

Subduction zones provide a splendid natural laboratory for the study of pressure-induced phase transformations and deep Earthquakes under nonhydrostatic stress. In subduction zones the lithosphere, Earth's cold boundary layer, is thrust deep into the mantle. Because the descending lithosphere is thick and a poor thermal conductor, it can remain anomalously cold for millions of years during active subduction. It may be as much as 1400 K cooler than the surrounding mantle. The primary geophysical expression of lower temperatures in subduction zones are extremaly deep Earthquakes.

To understand the subduction process it is necessary to look at the thermal regime of the Earth. The temperature within the Earth at first increases rapidly with depth, reaching about 1600 K at a depth of 100 kilometers. Then, it increases more gradually, approaching 2400 K at about 500 km.

In Fig. 1.6. we can observe the formation and subduction of the lithosphere (Toksoz, 1982). In Fig. 1.7. we have the world seismicity versus depth (Vassiliou, Hager and Raefsky, 1984).

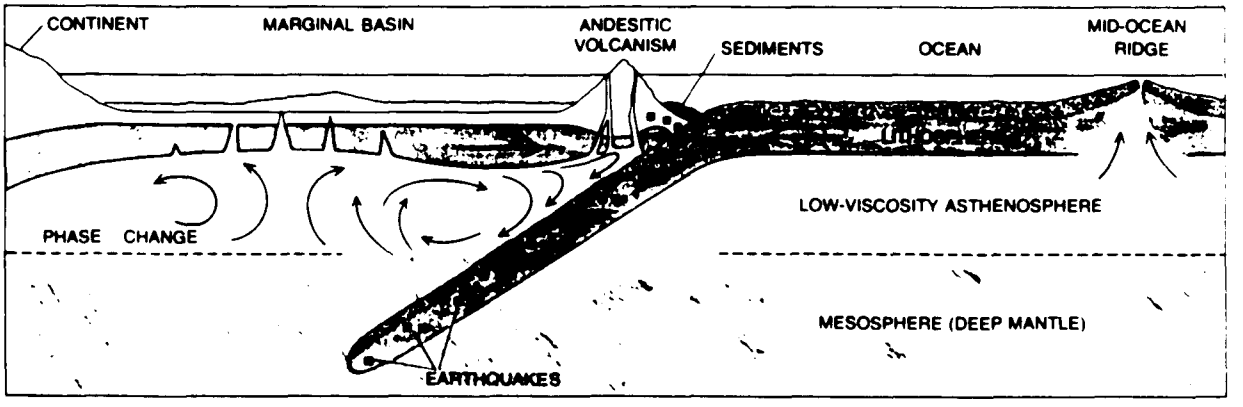


Fig. 1.6. Formation and subduction of lithosphere (Toksoz, 1982).

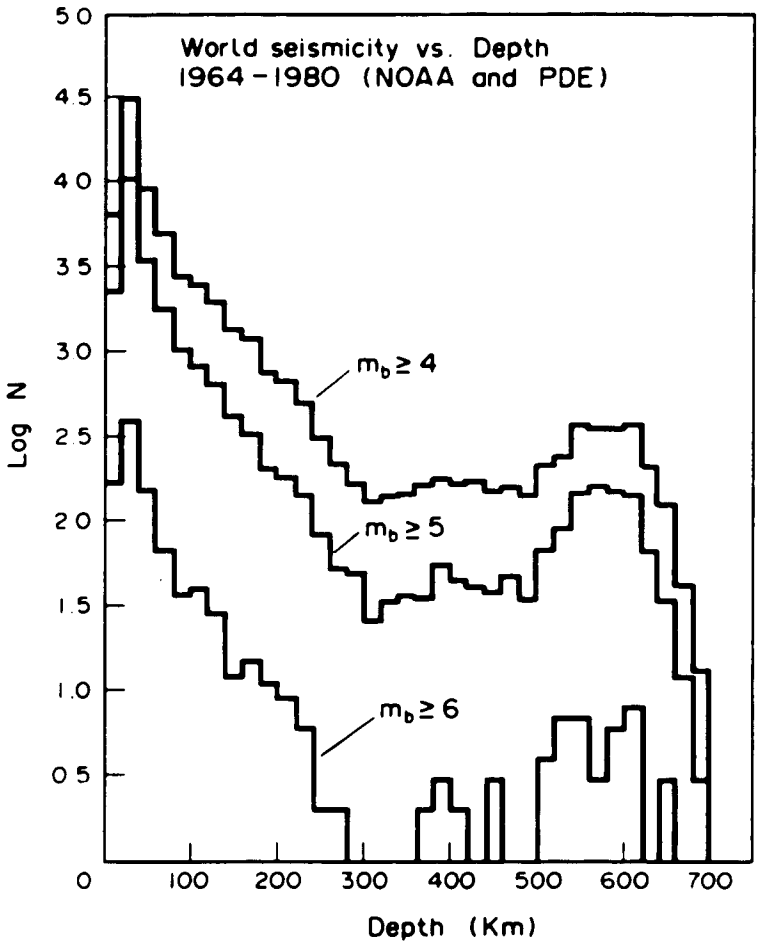


Fig. 1.7. Logarithm of the total number of earthquakes in the world versus depth, in 20 km intervals. The three curves are for different cutoff magnitudes $m_b$, the one-second body wave magnitude (according to Vassiliou, Hager and Raefsky, 1984).

## 1.5. Properties of the Earth's interior

The model of the Earth's interior that we can utilize for a description of a computer simulation of Earthquakes depends on many parameters which are: the maximum rock strength as a function of depth in the Earth, elastic constants as a function of pressure, density, shear velocity, temperature distribution with depth. These known parameters will be used to constrain our models of rock material and Earthquake processes. We need all these parameters to geophysical equations of state. At first, we shall apply the aforementioned parameters in order to develop constitutive equations of rock material with line defects. After that, these parameters will be utilized for describing of rock fracture under stresses comparable with the maximum rock strength. Finally, we shall use these parameters for the computer simulation of Earthquakes at different depths and for different mineral composition of focal zone.

In Fig. 1.8. we can see the maximum rock strength as a function of depth in the Earth for a quartz-rich sedimentary rock under a normal 20° C/km geothermal gradient and hydrostatic pore-fluid pressures. Higher thermal gradients or pore-fluid pressures would substantially reduce the strength, shifting the curves into the shaded region. Other rock materials show qualitatively similar behavior with a maximum

strength at the depth of transition between pressure-dependent brittle behavior and temperature-dependent plastic behavior (Suppe, 1989).

In Fig. 1.9. we review variations of elastic constants with pressure in the interior of the Earth (model data by Dziewonski et al., 1975).

Fig. 1.10. shows upper mantle velocities, density and anisotropic parameters in PREM. The dashed lines are the horizontal components of velocity (Dziewonski and Anderson, 1981).

In Fig. 1.11. we can observe the horizontal components of velocity and density in the PREM model.

Fig. 1.12. reviews a density profile of the Earth model by Dziewonski et al. (1975) (solid line) with corresponding extrapolated zero pressure (and room temperature) density (broken line).

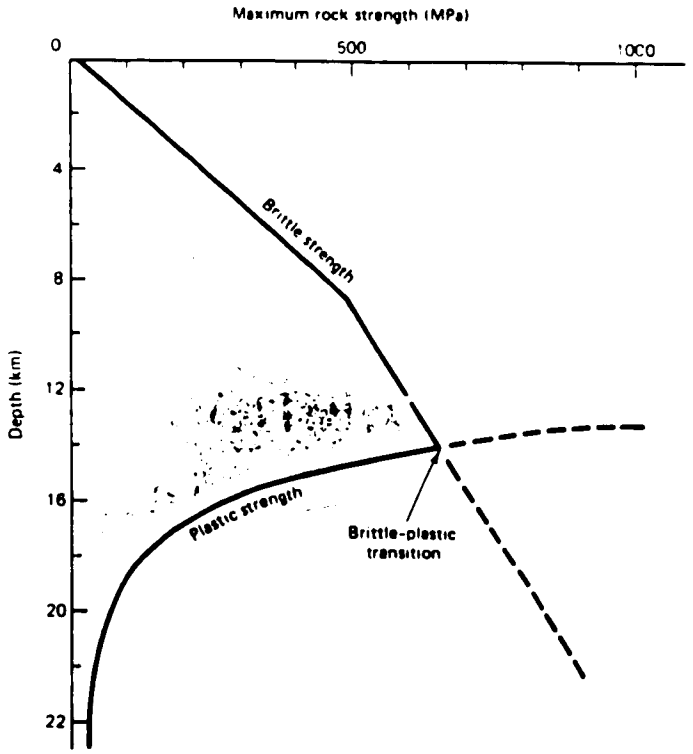


Fig. 1.8. Maximum rock strength as a function of depth in the earth for a quartz-rich sedimentary rock under a normal 20° C/km geothermal gradient and hydrostatic pore-fluid pressures. Higher thermal gradients or pore-fluid pressures would substantially reduce the strength, shifting the curves into the shaded region. Other rock materials show qualitatively similar behavior with a maximum strength at the depth of transition between pressure-dependent brittle behavior and temperature-dependent plastic behavior (Suppe, 1989).

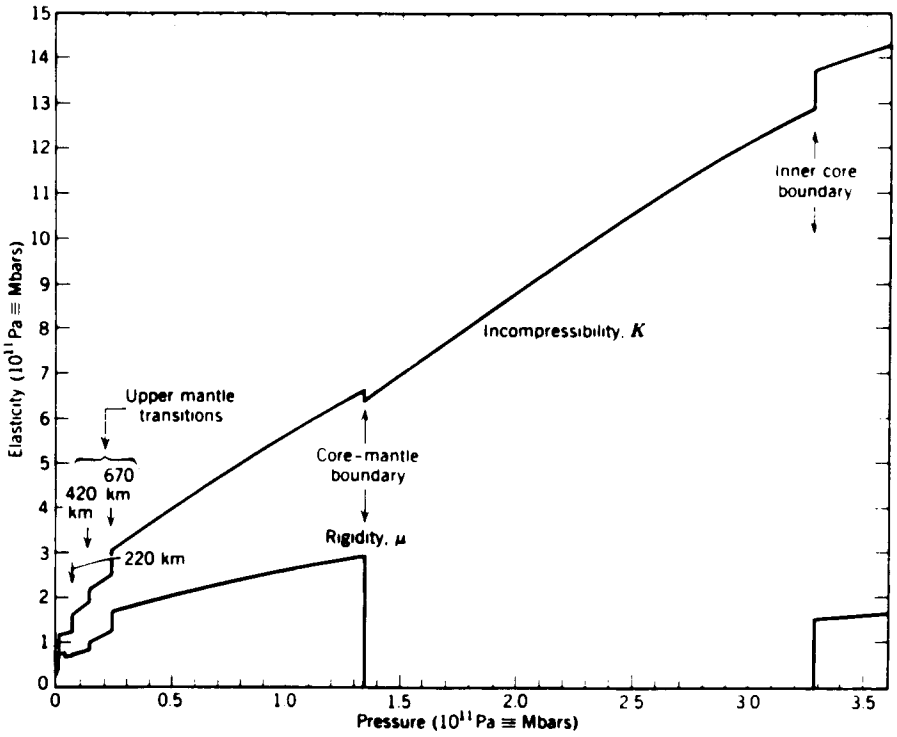


Fig. 1.9 Variations of elastic constants with pressure in the interior of the Earth (model data by Dziewonski et al. 1975).

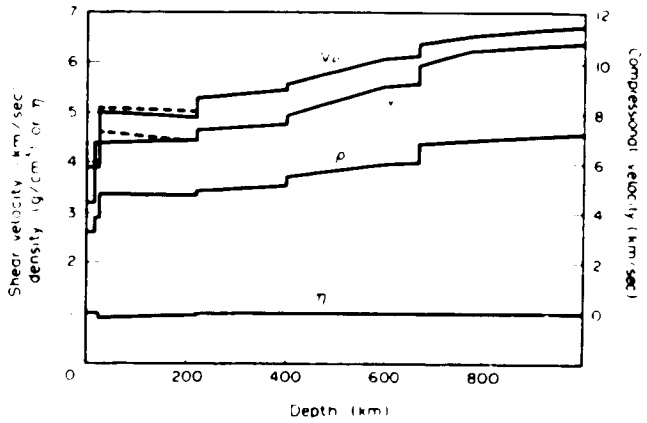


Fig. 1.10. Upper mantle velocities, density and anisotropic parameter in PREM. The dashed lines are the horizontal components of velocity. The solid curves are $\eta$, $\rho$ and the verical, or radial, components of velocity (Dziewonski and Anderson, 1981).

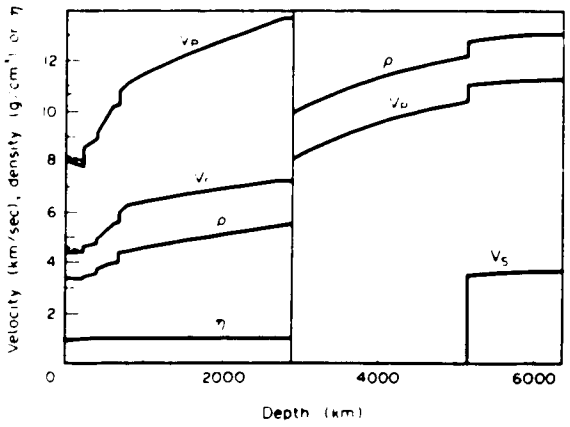


Fig. 1.11. The PREM model. Dashed lines are the horizontal components of velocity. When $\eta$ is 1, the model is isotropic. In this model the core is isotropic (Dziewonski and Anderson, 1981).

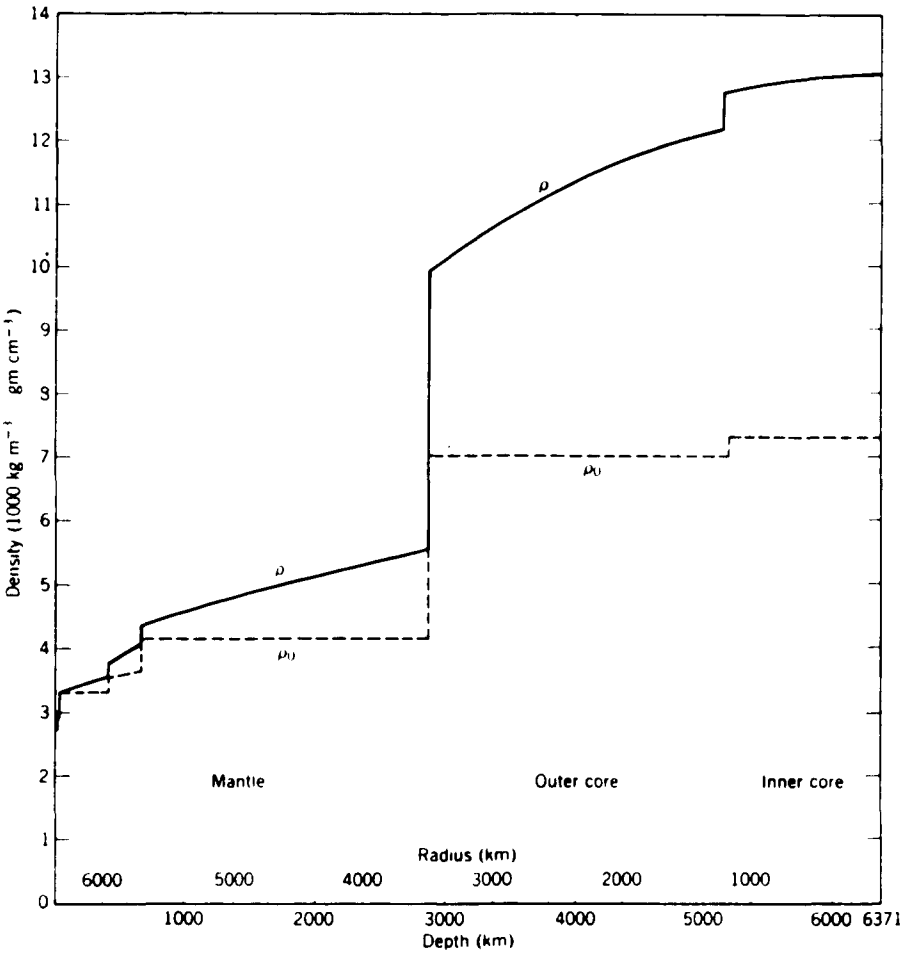


Fig. 1.12. Density profile of Earth model by Dziewonski et al. (1975) (solid line) with corresponding extrapolated zero pressure (and room teperature) density (broken line).

## 2. THERMODYNAMIC APPROACH TO EQUILIBRIUM

In static states it is possible to determine with greater precision, both from the macroscopic and from microscopic point of view, the spatial distribution of the component elements of a physical system and its cosequences. Static states are called states of thermodynamical equilibrium. It is from the macroscopic point of view that the thermodynamics of reversible processes describes with high precision the concept of equilibrium structures, such as crystal, for instance.

Let us now introduce the time factor into our considerations and deal with dynamic states in which the properties of a system vary in time. It follows from the second law of thermodynamics that there is spontaneous transition from dynamic states to states of thermodynamical equilibrium, i.e., to static ones. These static states are a kind of "attractors" to dynamic, i.e., nonequilibrium states. Boltzmann interprets statistically the second law of thermodynamics as implying that this tendency towards thermodynamical equilibrium is tantamount to the transition from less to more probable states. From the macroscopic point of view, he interprets this as transition from order to chaos. However, Boltzmann's interpretation applies to isolated systems, which cannot exchange either energy or mass with the

environment.

Let us now consider irreversible processes, i.e., those which occur only in one direction. Let us confine our considerations to irreversible (plastic) deformations of solids. We are going to specify a driving force in the process of irreversible deformation. In the context of the remark made in the Introduction on the non-existence of equilibrium state in any concentration of dislocations, we should say that the best approach to this problem would be to apply the thermodynamics of irreversible processes to it. However, nobody has done it up to now. The first attempt in describing of plastic deformations in the framework of thermodynamics of irreversible processes has been made by Bridgman (1950). He suggested a need for an extension of the fundamental concept of thermodynamics, namely the concept of entropy. Now, we come back to irreversible (plastic) deformations. It is worth noting that plastic deformations depend sensitively on shear stress but not on hydrostatic stress (pressure). The shear stress leads to shape changes but not to volume changes.

## 2.1 Thermal equilibrium

In equilibrium thermodynamics, states of equilibrium are characterized by the extreme values of certain functions (cf. Saxena, 1973) . For example, in a state of equilibrium the Helmholtz free energy has its minimum value. The Helmholtz free energy is defined as follows:

$$F = U - TS \qquad (2.1)$$

where U is the internal energy, T is the absolute temperature and S is the entropy. The Gibbs free energy is expressed by the formula:

$$G = H - TS \qquad (2.2)$$

where H = U + W is the enthalpy function and W is the work done by the external forces. Since thermodynamical equilibrium is a particular case of stationary states, it follows that those states can also be expressed by means of the extremal value of a certain function.

The problem of distinguishing between "reversible" and "irreversible" processes is usually described by the following inequality for entropy change:

$$dS \geq 0 \qquad (2.3)$$

In order to extend this formulation to open systems, we assume an additive decomposition of the entropy change dS, i.e., we assume the relation

$$dS = d_eS + d_iS \qquad (2.4)$$

where $d_eS$ represents an increase in entropy resulting from the transfer of entropy across the boundaries of the system and $d_iS$ is an increase in the entropy produced within the system. If we return to isolated systems in which $d_eS = 0$, the second law of thermodynamics in the form (2.3) will imply

$$dS = d_iS \geq 0 \ . \qquad (2.5)$$

The equality sign in the above relation applies to the state of equilibrium. It should be noted that $d_iS$ is the entropy production due to the irreversible processes occurring inside the system, such as a heat conduction, diffusion, chemical reactions and irreversible (plastic) strains (Majewski, 1984, 1986c, 1988; Mroz and Majewski, 1989).

Passing again to open systems, we should point out that they

are different from isolated ones in that that in the entropy change dS there appears a term representing the entropy flux $d_eS$. This term can be either positive or negative, and in the case of an isolated system it takes the value zero.

The classical formulation of the second law of thermodynamics for open systems requires that for an irreversible process, in view of (2.4), the following inequality should be satisfied:

$$d_eS + d_iS > 0 \quad . \qquad (2.6)$$

Thus, the classical formulation imposes the following conditions: if

$$d_eS < 0 \quad , \quad then \quad d_iS > | d_eS | \quad , \qquad (2.7)$$

and if

$$d_eS > 0 \quad , \quad then \quad | d_iS | < d_eS \quad , \; \forall \; d_iS \geq 0 \quad . \qquad (2.8$$

Thus, the classical concept admits the possibility of vanishing entropy change, i.e., the possibility $d_iS = 0$.

The local formulation of the second law of thermodynamics, on the other hand, excludes such a case, as it requires that the entropy production $d_iS$ should be positive whenever an irreversible process occurs. In the case just considered, this formulation requires that not only, according to the classical concept, equation (2.6) should be satisfied, but also that

$$d_iS \geq 0 \quad . \qquad (2.9)$$

The equality sign applies to a state of equilibrium. The local formulation of the second law of thermodynamics is thus an additional postulate introduced into the classical thermodynamics of irreversible processes. Namely, it is postulated that equation (2.4) applies not only to the system as a whole, as followed from classical thermodynamics, but also to its arbitrarily chosen "small" part. However, this "small" part must be sufficiently large to permit a phenomenological, i.e., macroscopic, method of description to be applied to it.

By inequality (2.9) the local formulation of the second law of thermodynamics implies that the entropy production $d_iS$ inside the system is positive or zero. This relation is very important for distinguishing between reversible and irreversible processes, as it is only in irreversible processes that the entropy production occurs. In addition, the second law of thermodynamics expresses very distinctly the

fact that irreversible processes advance in time in one direction, e.g., for an isolated system entropy is a function increasing monotonously in time. Functions of this type are very convenient for considering stability in the sense of Lyapounov (cf. Glansdorff and Prigogine, 1971). If, moreover, they satisfy some additional requirements defined for stability theory by Lyapounov, they are called Lyapounov functions.

For a function defining some physical states to correspond precisely to the requirements formulated in stability theory, some boundary conditions must be defined. In the opinion of Glansdorff and Prigogine (1971), entropy is exactly a Lyapounov function if it describes isolated systems. Moreover, under certain boundary conditions, such as imposed values of volume and temperature, also thermodynamic potentials such as the Helmholtz or Gibbs free energy can satisfy the conditions imposed by Lyapounov functions.

The stability conditions require the system to evolve to a state of equilibrium. As Planck noted in 1930, a state of equilibrium is an "attractor" for states of nonequilibrium. In addition, a state of equilibrium has the property that there is a thermodynamic potential for its description.

It should be stressed that the existence of a thermodynamic

potential is possible only in some cases. The local inequality (2.9) does not contain a total differential. In view of this, as was observed by Glansdorff and Prigogine (1971), it does not permit in general the determination of a Lyapounov function for this problem. On the whole, it is very difficult to determine Lyapounov functions.

As it is well known, the transition from equilibrium thermodynamics to that of irreversible processes involves difficulties in defining the fundamental thermodynamic quantities in states of nonequilibrium, e.g., the entropy production. The efforts to overcome these difficulties include, for instance, the postulate of the so-called "local equilibrium" (see Prigogine, 1969). Namely, it is postulated that even outside equilibrium the entropy depends only on the same variables as at equilibrium. In order to derive the expression for the entropy production, Prigogine (1969) introduced some additional assumptions. Namely, he assumed that he was determining the entropy production only in some neighborhood of equilibrium. He considered this neighborhood as a region of local equilibrium.

The corresponding theorem was formulated by Prigogine (1969, 1978): "for steady states sufficiently close to equilibrium entropy production reaches its minimun". It should be stressed that this theorem is valid within the linear thermodynamics of

irreversible processes where the Onsager reciprocity relations are satisfied. The validity of this theorem is an expression of the tendency of all systems, within the validity of the linear thermodynamics of irreversible processes, towards possibly low free energy dissipation, i.e., towards possibly close approach to thermodynamical equilibrium. For a long time attempts were made to extend the theorem of minimum entropy production to a situation further away from equilibrium. Finally, however, it turned out that at states far from thermodynamical equilibrium, the systems can behave in very different ways, even conversely to what follows from the theorem of minimum entropy production.

In summary, we should say that a similar situation takes place in the case of the minimum of the Gibbs free energy in thermodynamics of dislocations (see our remark in Introduction).

For our purpose here, we assume that the solid body under investigation may be treated as a closed thermodynamic system. In this body the internal energy U and entropy S of the body must fulfil the first law of thermodynamics in the form

$$U = Q + W \,, \qquad (2.10)$$

and the second law of thermodynamics in the form

$$S \geq \frac{Q}{T} \quad . \qquad (2.11)$$

Here Q denotes the heat and W denotes the work which is done on the body during and interchange with the surrounding. The equality sign describes thermal equilibrium or reversible process at a fixed temperature T. In the system considered, the mass is preserved.

From the aforementioned laws of thermodynamics we obtain

$$F \leq W \ , \qquad T = const. \qquad (2.12)$$

The above relations are well posed definition of entropy S and the Helmholtz free energy F which are defined in a state of equilibrium.

On the other hand, the Helmholtz free energy can be defined from the standpoint of microphysics by

$$F = - k T \ln Z \ , \qquad (2.13)$$

where k is the Boltzmann constant and Z is the partition function derived from the potential and kinetic energies of all the atoms comprising the solid body. The entropy can be

defined in such a way

$$S = - \frac{dF}{dT} \quad . \qquad (2.14)$$

In the thermodynamics of point and line defects we are not concerned with the free energy of the entire crystal. Our idealized model of the body consists of structural point and line defects and an ideal crystal. The considered free energy is that of all point defects, dislocations, boundaries and internal surfaces. Further we joint it with dislocations or as we will see, with defects in a dislocation superlattice.

## 2.2. Mechanical equilibrium

Mechanical equilibrium can be described as follows

$$dK_i = \sigma_{ij}\, n_j\, dA \ , \qquad (2.15)$$

where $dK_i$ denotes a component of the locally applied force dK, the vector n denotes the surface normal and dA denotes the area element at a point in which the stress is $\sigma_{ij}$. Moreover, the work done on an element of body is (Majewski, 1985a,b, 1986a,b, 1987, 1989, 1991a,b,c):

$$W = \int_{\theta} u_i\, dK_i \ , \qquad (2.16)$$

where $\theta$ denotes the surface of the body, and u is the displacement. We can write down the work W in the form

$$W = \frac{1}{2}\, V\, \sigma_{ij}\, e_{ij} \ , \qquad \delta W = V\, \sigma_{ij}\, \delta e_{ij} \ , \qquad (2.17)$$

where V denotes a volume.

In addition, we have for the mean values of strains

$$e_{ij} = \frac{1}{V} \int_{\theta} \frac{1}{2}\, (u_i\, n_j + u_j\, n_i)\, dA \qquad (2.18)$$

# PART 2

# RESULTS OF THE RESEARCH

## 3. THERMODYNAMIC RELATIONS IN A SUPERLATTICE

### 3.1. Basic definitions.

We introduce here the defect parameters which are defined by comparing the thermodynamic functions of a real crystal to a state that is free of defects. This is a typical approach for thermodynamics of defects. However, for linear defects like dislocations, we introduce a notion of an ideal body defined as follows. A continuum (or a crystal) contains a regular (cubic) superlattice of dislocation lines with a certain superlattice parameter $\Lambda$ (greater than the distance between atoms in an ordinary lattice). A real body contains defects (vacancies, irregularities) of a superlattice. We will join the thermodynamical function of line defects with the defects in a superlattice. With this assumption the Gibbs free energy may have a minimum corresponding to the equilibrium concentration of vacancies related to the vacant dislocation

lines in a superlattice. Formally many results can be now transferred from the thermodynamics of the point defects. The dislocation superlattice shall be related to some distribution of dislocations; their positions shall be in fact regarded as distributed randomly. Introducing this kind of ideal superlattice with regular distribution of dislocation lines we get a very rough approximation; a characteristic distance in such a superlattice - a superlattice constant $\Lambda$ shall be thus treated as a mean value of distances following from some random distribution of line defects. It is related to a dislocation density: $\alpha = b/\Lambda^2$ . How does construct a model of regular superlattice? Taking a real body with the $M^*$ dislocations we may add to it another m dislocations in such a way as a whole set of the ( $M^*$ + m ) dislocations fit to a regular superlattice of the dislocations ( $M^*$ + m = M ) with the smallest error. Such an error minimization procedure may give the best fitting value of m and hence also a value $M^*$. The number of line vacancies in this superlattice is evidently equal to m. For a dense distribution of dislocations the corresponding densities will be given as follows ($\Delta S$ denotes a surface of a cube approximating a body under consideration; m << M):

$$\alpha^{\circ} = \frac{\frac{b\,M}{3}}{\Delta S} = \frac{b}{\Lambda^2} \quad ,$$

$$\alpha = \frac{\frac{b\,M^{\circ}}{3}}{\Delta S} - \frac{b}{\Lambda^2}\left(1 - \frac{m}{M}\right) = \alpha^{o} - \mathfrak{a} \quad ,$$

$$\mathfrak{a} = \frac{\frac{b\,m}{3}}{\Delta S} = \frac{b\,m}{\Lambda^2\,M} \quad ,$$

where: $\alpha^{o}$ is a density of dislocation of a regular superlattice; $\alpha$ is a real dislocation density, $\mathfrak{a}$ is a density of line vacancies, b is a Burgers vector, $\Lambda$ is a constant of superlattice, $\Delta S = \Lambda^2\,M/3$. If a number m can be identified with an equilibrium value then it can be estimated independently (see consideration further on):

$$\mathfrak{a} = \frac{b}{\Lambda^2}\,\exp\left(-\frac{g^{f}}{k\,T}\right) \quad .$$

## 3.2 Thermodynamic functions for shear

To distinguish the thermodynamic function usually used in a case of compression tests with a work of external forces given by pdV we will use here symbols with a hat for a case of a pure shear work (under shear stress load) $\tau d\varepsilon$ with $d\varepsilon$ being an incremental in strain. Here $\tau V d\varepsilon$ is positive for work done by the external forces. We define quite formally the thermodynamic functions for work done by shearing enthalpy, Helmholtz and Gibbs free energies. Simply formal substitution $p \to \tau$, $V \to V\varepsilon$ (and for differential $dV \to V d\varepsilon$, for V = const.) changes these functions into shear functions: shear enthalpy, Gibbs free shear energy etc. However we shall add that those definitions and relations hold for V = const. and p = 0 (like thermodynamic functions for processes related to pressure action are defined for $\tau = 0$ and $\varepsilon = 0$). The thermodynamic shear functions will be marked by symbols with a hat. Thus for pure shear processes we have

$$\hat{U} = Q + \sigma V \varepsilon$$

We have here other definitions:

$$\textit{enthalpy} \qquad \hat{H} = \hat{U} + \tau V \varepsilon$$

$$\textit{Helmholtz energy} \qquad \hat{F} = \hat{U} - T S$$

$$\textit{Gibbs energy} \qquad \hat{G} = \hat{A} - T S \qquad (3.1)$$

We will consider here the external work dW related only to a pure shear action $\tau$ producing shear strain $\varepsilon$. We write down the first law of thermodynamics in the following form

$$\delta Q = d U - \tau V d \varepsilon \qquad (3.2)$$

A stress field is here defined by a derivative of external work

$$\sigma = \frac{1}{V} \frac{\partial \hat{W}}{\partial \varepsilon} \qquad (3.3)$$

whereas a resistance stress (e.g., in a crack motion) follows from the Helmholtz free energy (Kocks et al., 1975)

$$\tau = \frac{1}{V} \frac{\partial \hat{F}}{\partial \varepsilon} \qquad (3.4)$$

while a driving force (e.g., to move a crack) follows from a respective difference

$$\delta \psi = \delta \hat{W} - \delta \hat{F} \qquad (3.5)$$

$$\sigma - \tau = \frac{1}{V}\frac{\partial \psi}{\partial \varepsilon} \qquad (3.6)$$

In a constant temperature we have

$$\delta\psi = T\delta S - \delta \geq 0 \ ,$$

$$\delta \hat{W} \geq \delta \hat{F} \qquad (3.7)$$

where equilibrium (sign equal) expresses balance between an external force and a resistance one. For some processes a change of Gibbs free energy can be computed, especially when considering processes in which defect redistribution is involved. Hence for a given change of $\Delta\hat{G}$ we get a change in strain

$$\frac{\partial \Delta \hat{G}}{\partial \tau}\Big|_T = V\Delta\varepsilon \qquad (3.8)$$

and a change in entropy

$$\frac{\partial \Delta \hat{G}}{\partial T}\Big|_\tau = -\Delta S \qquad (3.9)$$

For equilibrium states we have:

$$S = \max; \quad T\delta S \geq 0 \ , \ for \ \delta Q = 0$$

$$F = \min; \quad \delta ( \hat{U} - T S ) = \delta \hat{F} \leq 0 \ , \ for \ \delta V = \delta T = 0$$

$$G = \min; \quad \delta ( \hat{U} + \tau V e - T S ) = \delta \hat{G} \leq 0 \ , \ for \ \delta \tau = \delta T =$$

For reversible processes with $\delta \hat{W} = \tau \delta (\varepsilon V)$ we have

$$\delta \hat{U} = T \delta S + \tau \delta (Ve) + \mathfrak{v} \delta M$$

$$\delta \hat{H} = T \delta S - V e \delta \tau + \mathfrak{v} \delta M$$

$$\delta \hat{F} = -S \delta T + \tau \delta (V e) + \mathfrak{v} \delta M$$

$$\delta \hat{G} = -S \delta T - V e \delta \tau + \mathfrak{v} \delta M \qquad (3.11)$$

where $\delta M$ is a change in number of line elements (dislocation vacancies) in a superlattice, while $\nu$ is a respective defect potential

$$\mathfrak{v} = \frac{\delta \hat{G}}{\delta M}\Big|_{\tau, T} \qquad (3.12)$$

The following Maxwell relations can be easily derived:

$$I) \quad \frac{\partial \tau}{\partial S}\Big|_{e_v} = \frac{\partial T}{\partial (Ve)}\Big|_S$$

$$II) \quad -\frac{\partial T}{\partial \tau}\Big|_S = \frac{\partial (Ve)}{\partial S}\Big|_\tau$$

$$III) \quad \frac{\partial S}{\partial (Ve)}\Big|_T = -\frac{\partial \tau}{\partial T}\Big|_{e_v}$$

$$IV) \quad \frac{\partial (Ve)}{\partial T}\Big|_\tau = \frac{\partial S}{\partial \tau}\Big|_T \qquad (3.13)$$

We can by analogy to the case of a body under pressure define the respective parameters related to shear processes, e.g.,

- a shear expansion coefficient:

$$\alpha = \frac{\partial e}{\partial T}\Big|_\tau \qquad (3.14)$$

- a rigidity (isothermal shear modulus):

$$\frac{1}{M} = \frac{\partial e}{\partial \tau}\Big|_T \qquad (3.15)$$

We can define here a thermal shear stress:

$$\tau_{th} = \int^{T} \frac{\partial \tau}{\partial T}\Big|_{e} dT \qquad (3.16)$$

The thermal shear stress is treated as the stress that appears in a medium during a process of heating from zero temperature up to temperature T under the constant strain

$$\frac{\partial \tau}{\partial T}\Big|_{e} = \mu \alpha \qquad (3.17)$$

Now, the thermal shear stress takes the form

$$\tau_{th} = \int^{T} \mu \alpha \, dT \qquad (3.18)$$

From relation (3.11) we obtain for an isothermal process

$$d\hat{G} = -eV d\tau \qquad (3.19)$$

or alternatively

$$d\hat{G} = -\mu e V \, de \qquad (3.20)$$

Rigidity dependence on shears can be found as follows:

$$\frac{\partial \mu}{\partial \tau}\Big|_{T} = \frac{\partial \mu}{\partial e}\Big|_{T} \quad \frac{\partial e}{\partial \tau}\Big|_{T} = \frac{\partial \mu}{\mu \partial e}\Big|_{T} \quad hence \quad d\mu = \mu \frac{\partial \mu}{\partial \tau}\Big|_{T} de$$

$$\Lambda \quad d\,(\varepsilon\mu) \;=\; \mu d\varepsilon + \varepsilon d\mu \;=\; \mu\,(1 + \frac{\partial\mu}{\partial\tau})\,d\varepsilon \quad .$$

From the last relation follows immediately

$$\mu\, d\varepsilon \;=\; \frac{d(\mu\varepsilon)}{(1 + \frac{\partial\mu}{\partial\tau}|_T)} \qquad (3.21)$$

From (3.20) we obtain in the case of T = const.

$$d\hat{G} \;=\; \frac{-V\,\varepsilon d(\mu\varepsilon)}{(1 + \frac{\partial\mu}{\partial\tau})}|_T \qquad (3.22)$$

This equation plays a fundamental role in the formulation of the model of line defects.

# 4. STATISTICAL APPROACH TO EQUILIBRIUM

A statistical approach to line defects at an equilibrium state is quite different from that one for a case of the point defects. The Gibbs function for a crystal containing the line defects (dislocations) can be written as follows

$$\hat{G} = \hat{G}^{o} + m\hat{g} - T\hat{S}_{c}$$

where m are the line defects (dislocations); $S_c$ is a configurational entropy.

We shall underline here that formation of a dislocation gives negative contribution to Gibbs energy (Kocks et al. 1975) and therefore it is not possible to find a minimum of the Gibbs function in respect to a number of dislocations (Ranalli, 1987). However, when introducing here the concept of a superlattice and the line vacancies in it, we can get a situation similar as in the point defects: there exists a minimum of the Gibbs function corresponding to a state of equilibrium distribution of defects. We shall note that in many futher considerations we will follow the approach given by Varotsos and Alexopoulos (1986) in thermodynamics of the point defects.

Now we can rewrite the above given equation such that

$$\hat{G} = \hat{G}^{o} + m\hat{g}^{f} - T\hat{S}_{c} \qquad (4.1)$$

where m is a number of line vacancies in a superlattice, $\hat{g}^{f}$ is a formation energy for line vacancy, $\hat{S}_{c}$ is a configuration entropy of line vacancies.

Considering a regular superlattice with M′ lines crossing one face of a cube we have a total number of the line defects (dislocatons) M = 3M′ forming an ideal superlattice. In a given shear field oriented conformly to a normal of a face of such a cube we will deal with M′ edge dislocations and 2M′ screw dislocations*. Referring to the known expressions for the values of self-energies of dislocations we can estimate an average value e of self-energy of any dislocations considered as equal to

$$e = 1.111\, e_{screw} \qquad (4.2)$$

for $\nu = 0.25$; here $e_{screw}$ denotes the self-energy of a screw dislocation.

---

(*) Note that the Burgers's and tangent vectors are parallel for a screw dislocation in contrast with edge dislocations; therefore, it has no slip plane. It is called a screw dislocation because the atomic planes spiral around the dislocation.

An existence of a superlattice could be 'a priori' related to some values of strength parameters. We can consider different cases:

I - ideal superlattice probably relates to minimum yield stress value,

II - real superlattice relates to actual shear strength,

III - ideal crystal (no line defects, no superlattice); here strength would be equal to theoretical value of $\mu$.

Following Varotsos and Alexopoulos (1986) we can now define by m a number of line vacancies and by M a total number of line dislocations (forming superlattice). Then, a configuration entropy equals

$$\hat{S}_c = k \ln \frac{(M + m)!}{M!\,m!}$$

For an equilibrum state under constant local shear $\tau$ and temperature T the Gibbs energy reaches minimum, hence an equilibrium value could be found

$$\frac{\partial \hat{G}}{\partial m}\Big|_{\tau,T} = 0 \qquad (4.3)$$

defining a number of vacancies in an equilibrium state.
We get

$$m = M \exp\left(-\frac{\hat{g}^f}{nT}\right)$$

$$\hat{S}_c = m\left(k + \frac{\hat{g}^f}{T}\right) \qquad (4.4)$$

while a Gibbs energy function becomes

$$\hat{G} = \hat{G}^\circ - mkT \qquad (4.5)$$

The equilibrium free energy is less than that for an ideal superlattice $\hat{G}^\circ$ by energy kT per line vacancy.
For entropy we get in a similar way

$$\hat{S} = \hat{S}^\circ + m\left(\hat{S}^f + k + \frac{\hat{g}^f}{T}\right)$$

$$\hat{S}^f = -\frac{\partial \hat{g}^f}{\partial T}\Big|_\tau \qquad (4.6)$$

and for enthalpy

where $\hat{g}^f + T\hat{S}^f = \hat{h}^f$ is a formation enthalpy.

$$\hat{H} = G^{o} + TS^{o} + m(\hat{g}^{f} + T\hat{s}^{f}) \qquad (4.7)$$

Finally, for a strain change we get (V = const.):

$$\varepsilon = -\frac{1}{V}\frac{\partial G}{\partial \tau}\Big|_{T} = -\frac{1}{V}\frac{\partial G^{o}}{\partial \tau}\Big|_{T} + kT\frac{\partial m}{\partial \tau}\Big|_{T} \qquad (4.8)$$

$$\varepsilon = \varepsilon^{o} + m\frac{\partial \hat{g}^{f}}{\partial \tau}\Big|_{T} \qquad (4.9)$$

the Helmholtz free energy can be similarly to (2.13) expressed by partition function for all dislocations in a superlattice $\hat{Z}$:

$$\hat{F} = -kTm\hat{Z} \qquad (4.10)$$

## 5. FORMATION OF LINE DEFECTS (VACANCIES)

In this approach we compare the thermodynamic functions $\hat{G}$, F, $\hat{A}$, $\hat{S}$ of the real crystal with the corresponding functions $\hat{G}^{\circ}$, $F^{\circ}$, $\hat{A}^{\circ}$, $\hat{S}^{\circ}$ of an idealized superlattice without line defects (regular lattice of line defects without line vacancies).

In a crystal with single line defects we cannot find a defect distribution close to the state of an equilibrium. We assume that the perfect superlattice is close enough to an equilibrium in order to define some thermodynamic functions for such body.

We denote by $\hat{g}^{f}$ the formation Gibbs free energy for a line defect (vacancy in superlattice).

Varotsos and Alexopoulos (1986) have introduced the so-called CB$\Omega$ theory approximating a contribution to the Gibbs energy from formation of a point defect; the assumption was made that this contribution is proportional to a product B$\Omega$ (where B = 1/K, B - bulk modulus, K - compressibility and $\Omega$ - mean atomic volume).

Extrapolating their theory to a case of line defects (vacancies in a superlattice) we assume that a similar contribution can approximate a formation Gibbs energy $\hat{g}^{f}$ of

line defect (vacancy).

If we consider a pure shear elastic deformation, we obtain an elastic energy

$$U = \varepsilon\tau V = 2\mu\varepsilon^2 V \qquad (5.1)$$

*For the case when* $\frac{\partial\mu}{\partial\tau}|_T = 0$ *we obtain* (3.22):

$$d\hat{G} = -V\varepsilon d(\mu\varepsilon) \qquad (5.2)$$

For any irreversible motion of defects, like fracture area increase, or crack extension, we can discuss a degree of deviation from an equilibrium state, its measure will help us to define the driving forces (Kocks et al, 1975).
For T = const we define such deviation by the following way

$$\delta\psi \equiv T\delta S - \delta Q = \delta W - \delta F \qquad (5.3)$$

$$\delta\psi > 0 \qquad (\delta T = 0) \ .$$

Work done by extremal forces equals $\delta W = V\sigma\ \delta\varepsilon$ and we get for an equilibrium state $\delta F = V\sigma\ \delta\varepsilon$ $(\delta\sigma = 0)$. It is therefore reasonable to define a shear resistance as follows

$$\tau \equiv \frac{1}{V}\frac{\delta F}{\delta e} \qquad (5.4)$$

hence, a driving force becomes according to (5.3)

$$\frac{1}{V}\frac{\delta \psi}{\delta e} \equiv \sigma - \tau \qquad (5.5)$$

for a dislocation glide over a surface element $\delta a$ with the Burgers vector b we get from (2.17), (2.18):

$$\delta e = \frac{b\delta a}{V} \qquad (5.6)$$

Hence, we have immediately the following relations

$$\sigma \equiv \frac{1}{b}\frac{\delta W}{\delta a}\ ,\ \tau \equiv \frac{1}{b}\frac{\delta F}{\delta a}\ ,\ b(\sigma - \tau) = \frac{\delta \psi}{\delta a} \qquad (5.7)$$

If $\sigma > \tau$ we have a gliding motion, however for $\tau > \sigma$ we may observe a glide event according to thermal fluctuations.

If we have two equilibrium positions, stable and unstable, related to surface $a_s$ and $a_n$ respectively, then for a difference in free energies we get

$$\Delta G = -\int_{a_s}^{a_n} (\sigma - \tau)\, b\, da = -\int_{\tau}^{\sigma} b \Delta a\, d\tau \qquad (5.8)$$

The probability that thermal energy fluctuation become greater than $\tau$ is expressed as follows

$$p = \exp \frac{-\Delta G}{KT} \qquad (5.9)$$

The self-energy per dislocation length amounts to

$$F_{screw} = \frac{\mu b^2}{2} \ln \frac{L}{r^o}$$

(for characteristic distance L = 500 V) and

$$F_{edge} = \frac{1}{1 - \nu} \quad , \quad F_{screw} \approx 1.33 F_{screw} \quad (\nu = 0.25).$$

For different shape of dislocation, for arrays of piled-up dislocations there are different self-stresses. This problem in a detail way is discussed by Kocks et al. (1975).

A dislocation motion V (mass neglected) is given by the drag coefficient B

$$B\hat{V} = b(\sigma - \tau) \qquad (5.10)$$

where $B \approx kT/\Omega\omega_A$, and $\omega_A$ is an atomic frequency ($\omega_A \equiv V_s/b \approx 10^{13}$ $s^{-1}$) and $\Omega$ is an atomic volume.

The coefficient B takes the following values for metal and ionic crystals

$$10^{-4} \wedge 10^{-5}\left[\frac{N\,s}{m^2}\right] \quad , \quad (10^{-3} - 10^{-4}\left[\frac{dyn\ sec}{cm^2}\right]) \quad .$$

Formation of a surface element da by a dislocation with the Burgers vector b brings a contribution to the Gibbs function - $\sigma$b da. Conversely, formation energy of a vacancy in a dislocation superlattice will be positive: b da (work done d W = $-\sigma$ b d a).

Thus, under stress load $\sigma$ we put for Gibbs function related to an existing dislocation

$$G = U - TS - \sigma ba$$

and correspondingly for one line vacancy in a superlattice ($\Lambda$ is a superlattice constant)

$$\hat{G} = \hat{U} - T\hat{S} + \sigma ba \quad ; \qquad \hat{G} = \hat{U} - T\hat{S} + \sigma b\Lambda^2 \qquad (5.10)$$

or

$$\delta\hat{G} = \sigma b\Lambda^2\delta m \qquad (5.11)$$

where $\delta$m is a change in number of line vacancies. We assume here that all functions, including energy, relate to a unit of dislocation line.

This consideration allows us to postulate an approximate approach to thermodynamics of line defects in a superlattice. We assume that a formation energy $\hat{g}^f$ for a line defect (a vacancy in a superlattice) is related to product $\mu b\Lambda^2$ ($\mu$ - rigidity , $b = \Delta u$ is the Burgers vector of dislocation):

$$\hat{g}^f = d\mu b\Lambda^2 \quad . \qquad (5.12)$$

where d is a proportionality constant (it is assumed that it does not depend on stress load $\sigma$).

This assumption refers to the CB$\Omega$ - model presented in many papers of Alexopoulos and Varotsos (comp. monograph by Varotsos and Alexopoulos, 1986).

Many relations proved in their papers can be formally transfered here by substitutions:

$$V \to eV, \quad p \to \sigma, \quad B \to \mu, \quad \omega \to b\Lambda^2 \quad . \qquad (5.13)$$

# 6. THERMODYNAMIC APPROACH TO THE REBOUND THEORY OF DISLOCATION PROCESSES

The evolution equations of the rebound theory for the in-plane (shear and tensile) motion are given as follows (Teisseyre 1985a,b, 1987);

$$(\tau - \tau_F)\ [(\tau - \tau_F)^2 + (\sigma - \sigma_C)^2] = C_1 v \left(\frac{d\tau}{dx} - \frac{d\sigma}{dy}\right)$$

$$(\sigma - \sigma_C)\ [(\tau - \tau_F)^2 + (\sigma - \sigma_C)^2] = -C_1 w \left(\frac{d\tau}{dx} - \frac{d\sigma}{dy}\right) \qquad (6.1)$$

where $\tau$ and $\sigma$ are the shear and tensile stresses; $\tau_F$, $\sigma_C$ are the friction and cohesion resistance stresses; v, w are velocities of the bulk dislocations in the x and y directions, respectively.

To solve the system for four unknown functions $\tau$, $\sigma$, v, w we supplement the system by the energy rate balance:

$$\dot{E}_k + \dot{E}_p = - L_C - L_F \qquad (6.2)$$

where $E_k$ is kinetic, $E_p$ is potential energy, $L_C$ is the rate of work needed to create a crack of unit surface, and $L_F$ is the rate of frictional work.

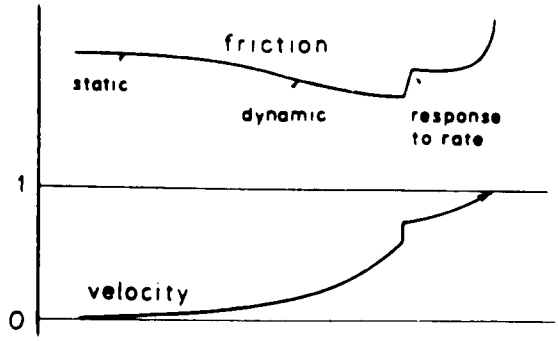


Fig. 6.1. Velocity and velocity rate dependent friction: schematic diagram (after Teisseyre, 1987).

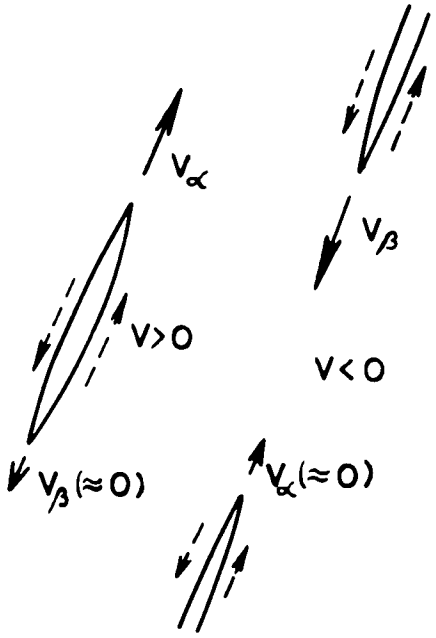


Fig. 6.2. Extension of crack (left diagram) and crack joining in rebound motion V<0 (right diagram) - a case of the in-plane shear cracks (after Teisseyre, 1987).

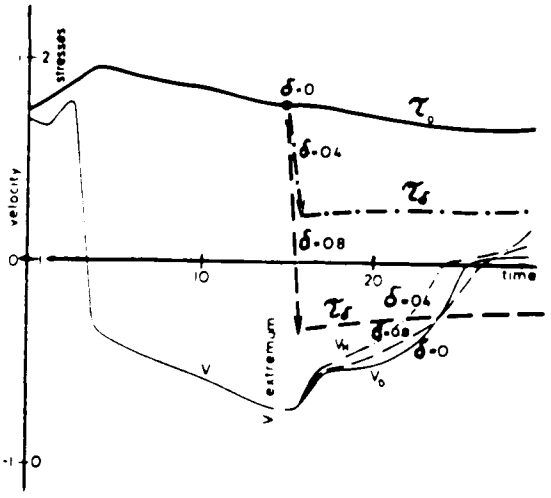


Fig. 6.3. Stresses and stress drops (double lines) for different $\delta$ values; stresses in relative ($\tau/\tau_{regional}$) conventional scale ($5\tau_{regional}=1$), velocity in shear wave velocity unit, time in conventional scale (after Teisseyre, 1987).

The rebound theory of Earthquakes has been developed by many authors. Recently, a very important contribution to this theory has been provided by Teisseyre (1985a,b, 1987). All these papers were discussing the rebound Earthquake theory in the context of pure mechanical approach, however, they included dislocations as well. In the framework of isothermal theory we can estimate behavior of rock material in Earthquake process. Namely, we can determine characteristic features of this process. First of all, we face an extention of crack and crack merging in rebound motion. Such an example of extention of crack and crack merging for a case of the in-plane shear cracks is shown in Fig. 6.2. This figure is a very typical example of crack behavior and generating of dislocations at the ends of cracks. This relationship and interactions between cracks and dislocations are described in detail by Teisseyre (1987). Moreover, Teisseyre (19787) also determined a velocity and velocity rate dependent friction in rebound motion which is presented in Fig. 6.1. We should emphasize that the energy release and stress drop are estimated as two main parameters of an Earthquake event. Such an example of stresses and stress drops are shown in Fig. 6.3 (after Teisseyre). He presented also the velocity in rebound motion in the same diagram. He assumed that the region considered is already under some regional stress. All the aforementioned features of Earthquakes can be described on the base of the rebound Earthquake theory without thermal considerations.

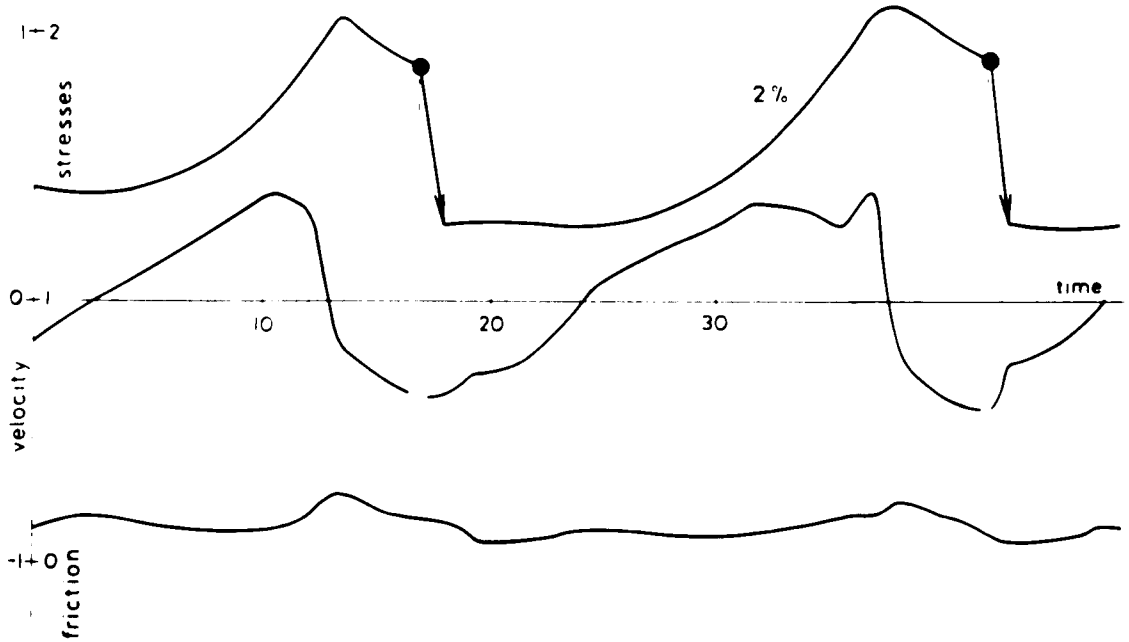


Fig. 6.4. Fragment of an earthquake sequence for 2% increase of regional stress field per unit time; stresses and friction in relative conventional scale, for stresses $5\tau_{regional}=1$, for friction $10\tau_{regional}=1$, velocities in shear wave velocity unit (after Teisseyre, 1987).

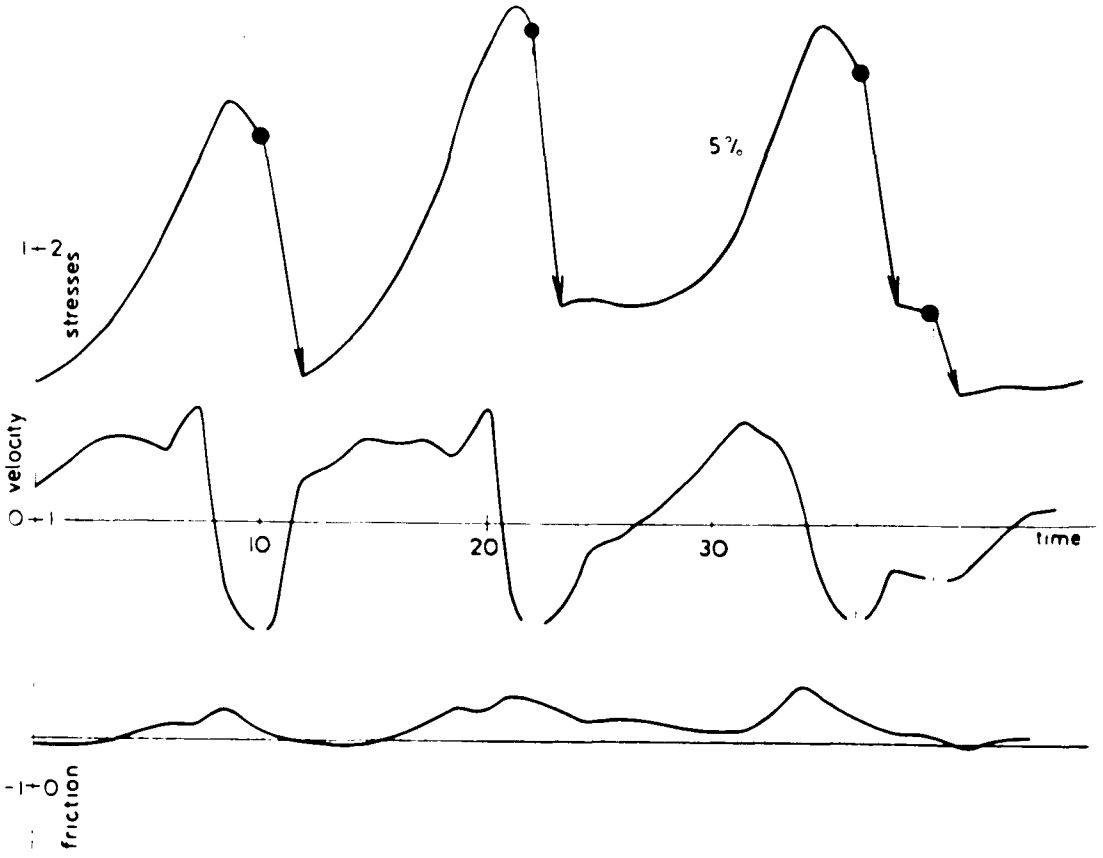


Fig. 6.5. Fragment of an earthquake sequence for 5% increase of regional stress field per unit time, scale and units as in Figs. 6.3 and 6.4 (after Teisseyre, 1987).

In the framework of the same isothermal rebound theory it is possible to determine an Earthquake sequence. Such a fragment of an Earthquake sequence for 2% increase of regional stress field per unit time is presented in Fig. 6.4 (after Teisseyre, 1987). We can observe the stresses and velocities and friction in rebound motion as functions of time. Another example of fragment of an Earthquake sequence but for 5% increase of regional stress field per unit time is presented in Fig. 6.5 (after Teisseyre, 1987). During an Earthquke process we have very often such a situation that the stress level is constant but strains are still increasing. We call it the creep process. In the rebound motion both the Earthquke and creep energies are very important for describing the process of deformation. In Fig. 6.6 we can observe the sums of the Earthquake and creep energies in time. We can see double quakes, creep, quakes and calm fragments of Earthquke process.

All these results from Fig. 6.1 to 6.6 were obtained by Teisseyre (1987) in the framework of pure mechanical Earthquke rebound theory. Our goal is to introduce a temperature dependence to this theory in order to develop a general theormodynamic approach to the rebound theory of dislocation processes.

The corresponding motions (after introducing a temperature

dependence), can be written by the following system which describes a thermo-mechanical coupling:

$$\tau(\tau + \tau_F)^2 = C_1 v \left(\frac{d\tau}{dx} - \frac{d\sigma}{dy}\right)$$

$$\sigma(\sigma + \sigma_C)^2 = -C_1 w \left(\frac{d\tau}{dx} - \frac{d\sigma}{dy}\right) \qquad (6.3)$$

$$\frac{\partial}{\partial t}\left[\frac{1}{2}\varrho\left(\frac{\partial u}{\partial t}\right)^2 + \frac{1}{4\mu}\left(\tau^2 - \frac{\nu}{1+\nu}(tr\tau)^2\right) +\right.$$

$$\left.\kappa(T - T_o)\, tr\,\tau\right] = -v(1 - v^2)^{-\frac{1}{2}} K^2 \alpha_c - v\tau_F \alpha\,[1 +$$

$$\left.\gamma\,(T - T_o)\, C_p\right] \qquad (6.4)$$

where T is an absolute temperature, while $T_o$ is its reference value (corresponding to a case of no stress load); $C_p$ denotes the specific heat for the constant pressure (the pressure is constant at a particular depth in the Earth's interior); K denotes the stress intensity factor; $C_1$ is a material constant; $\kappa$ denotes a thermal conductivity.

The left-hand side represents the rate of kinetic and strain energies, while the right-hand side describes terms related to a material flow.

To close a system containing dependence on temperature we shall add the heat conductivity Fourier equation:

$$\kappa \nabla^2 T = C_p \dot{T} + T_o \left(\lambda + \frac{2}{3}\mu\right) \gamma_o \frac{d}{d\xi} \left(v\tau + \frac{1}{3} w\sigma\right)$$

where $\kappa$ is a thermal conductivity coefficient, $c_p$ is a specific heat for a constant pressure p, $\alpha_o$ is a thermal volume expansion coefficient. In the above equation it is assumed that material modulus $\mu = \lambda = 1$.

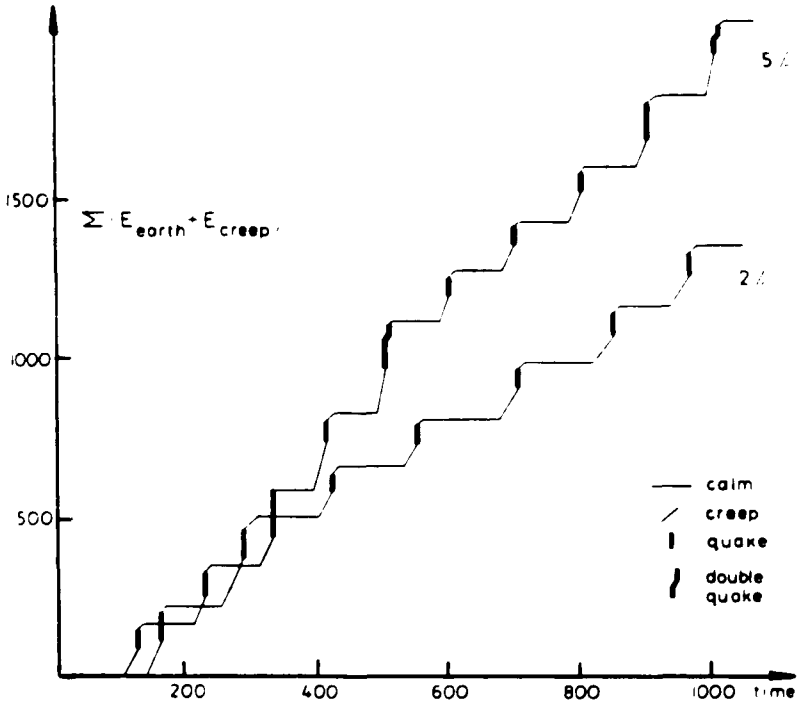


Fig. 6.6. Sums of the earthquake and creep energies; energy and time in conventional scales (after Teisseyre, 1987).

## 7. THERMODYNAMICAL APPROACH TO THE ROCK FRACTURE

Now, we will recall the Orowan relation for macroscopic viscoplastic strain rate

$$v_{dislocation} = b \dot{\alpha} L = b \alpha_f v_f \quad ,$$

where b denotes the Burgers vector, the time derivative of $\dot{\alpha}$ denotes a velocity of dislocation density, L denotes an average distance between obstacles in dislocation motion, $\alpha_f$ denotes a dislocation density for glide motions of dislocations, and $v_f$ denotes a velocity of dislocation jump between obstacles for glide motions of dislocations. In such a case, the macroscopic strain rate for the medium with cracks and dislocations, can be written as follows

$$V = V_{dislocation}[1 + \alpha_c (g^m + g^{act}) C_2]$$

where $\alpha_c$ denotes a crack density, and $C_2$ denotes a material constant.

Now, we postulate a defect Gibbs free energy for a unit length of linear dislocation in the form

$$g = d \mu b \Lambda^2$$

where g denotes a defect Gibbs free energy and in a case of

linear defect formation it will take a form of $g^f$ which denotes a defect formation Gibbs free energy, and in a case of activation process it will take a form of $g^{act}$ which denotes a defect activation Gibbs free energy, in addition, in a case of defect motion it will take a form of $g^m$ which denotes a defect motion Gibbs free energy.

Moreover, we postulate an additive decomposition of the time derivative of crack density

$$\dot{\alpha}_c = \dot{\alpha}_{c(formation)} + \dot{\alpha}_{c(growth)} + \dot{\alpha}_{c(activation)} + \dot{\alpha}_{c(fracture)}$$

where the part of crack density rate responsible for a crack formation is postulated in the form

$$\dot{\alpha}_{c(formation)} = C_3 \, g^f \, \alpha \, \dot{t} + C_4 \, (g^f + g^{act}) \, \frac{\alpha}{3} \, tr\dot{t}$$

where $\alpha$ denotes a dislocation density, and the part of cracks density rate responsible for existing crack growth is postulated in the form

$$\dot{\alpha}_{c(growth)} = (\alpha_c^{max} - \alpha_c) \, \alpha \, (tr\mathbf{M}) \, (g^{act} + g^m) \, v$$

where $\alpha_c^{max}$ denotes the maximum value of cracks density, and M denotes a second-order tensor, and V denotes a macroscopic strain rate of the medium with cracks and dislocations which

was determined by previous formula. In addition, the part of crack density rate due to activation processes is postulated in the form

$$\dot{\alpha}_{c(activation)} = C_5\, g^{act}\, \alpha$$

Here $C_3$, $C_4$, $C_5$, $C_6$ are material constants.

The last stage of deformation process is characterized by the merging of cracks and fracture within rock material. The part of crack density which is responsible for a rock fracture is

$$\dot{\alpha}_{c(fracture)} = C_6\, (g^{m} + g^{act})\, \alpha\, \langle \alpha_c - \alpha_c^{o} \rangle$$

where $\alpha_c^{\circ}$ denotes the critical value of $\alpha_c$. Above this value we deal with process of fracture. Below this value we deal with continous deformation of rock. This special kind of brackets < x > is defined in the following way

$$\langle \alpha_c - \alpha_c^{o} \rangle = 0 \qquad if \qquad \alpha_c \le \alpha_c^{o}$$

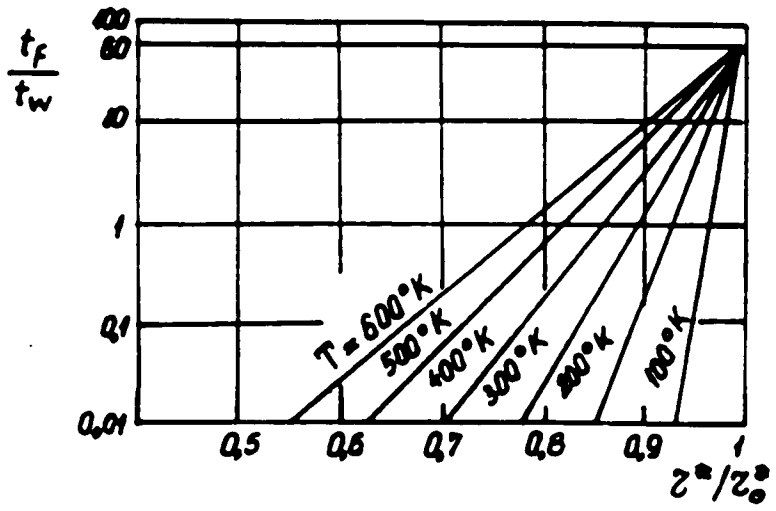


Fig. 7.1. Log $(t_F/t_w)$ versus effective stress for polycrystalline olivine with grain size 0.1 mm at different temperatures.

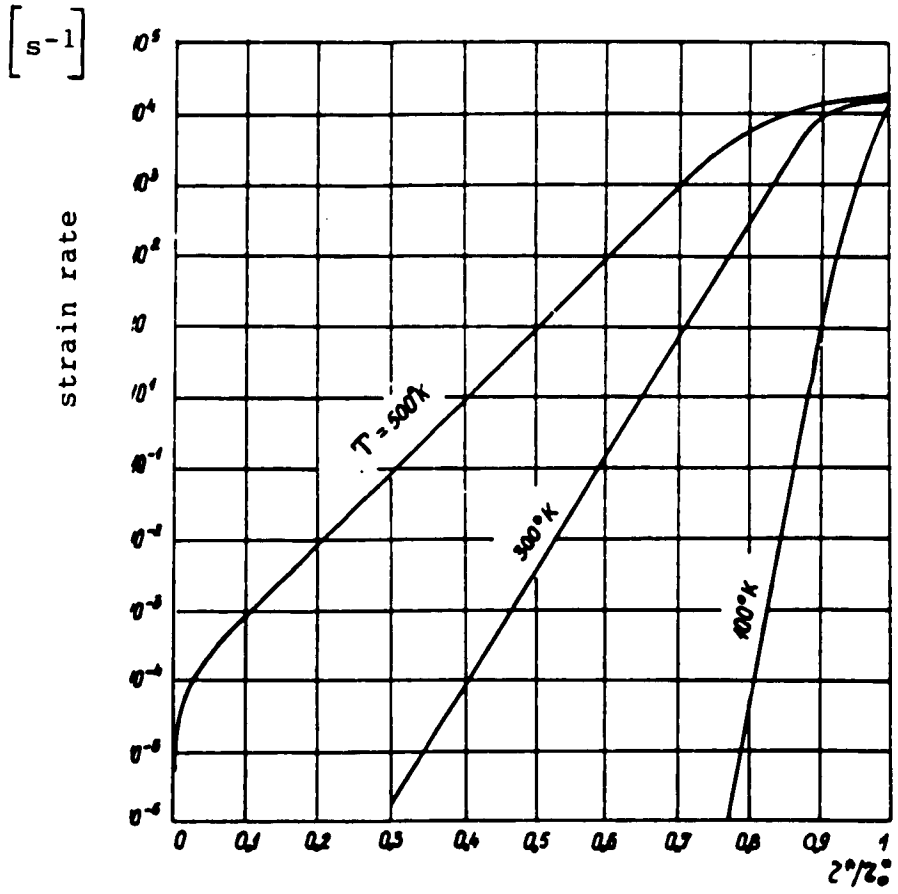


Fig. 7.2. Logarithm of the strain rate versus effective stress for polycrystalline olivine with grain size 0.1 mm at different temperatures.

$t_F$, which is required for the motion from the previous obstacle to the next one. If $l_F$ denotes a mean distance between two consecutive obstacles, then a mean velocity of dislocation is equal to

$$v = \frac{l_F}{t_w + t_F} \qquad (7.14)$$

During a motion of dislocation we have the following relation for a unit of length of dislocation

$$v_F B = \tau^* b \qquad (7.15)$$

where B is a coefficient of hampering. The value of B is equal to $10^{-5}$ cgs at the temperature 4.2° K and it is equal $10^{-4}$ cgs at the room temperature. The strain rate can be expressed by the relationship

$$\epsilon = b^2 \alpha_M \nu_D \left(\exp\left[\frac{(\Delta g - \tau^* \Delta V^*)}{k T} + \frac{\nu_D B}{\tau^*}\right]\right)^{-1} \qquad (7.16)$$

where $\alpha_M$ denotes a density of all mobile dislocations. In the expression for temperature we can neglect the term which describes jumps of dislocations to the back and we obtain so-called reduced temperature. In the expression for the effective stress we can drop the jump dislocation time because it is negligible in comparison with the waiting time of dislocation. In this way we obtain the reduced effective

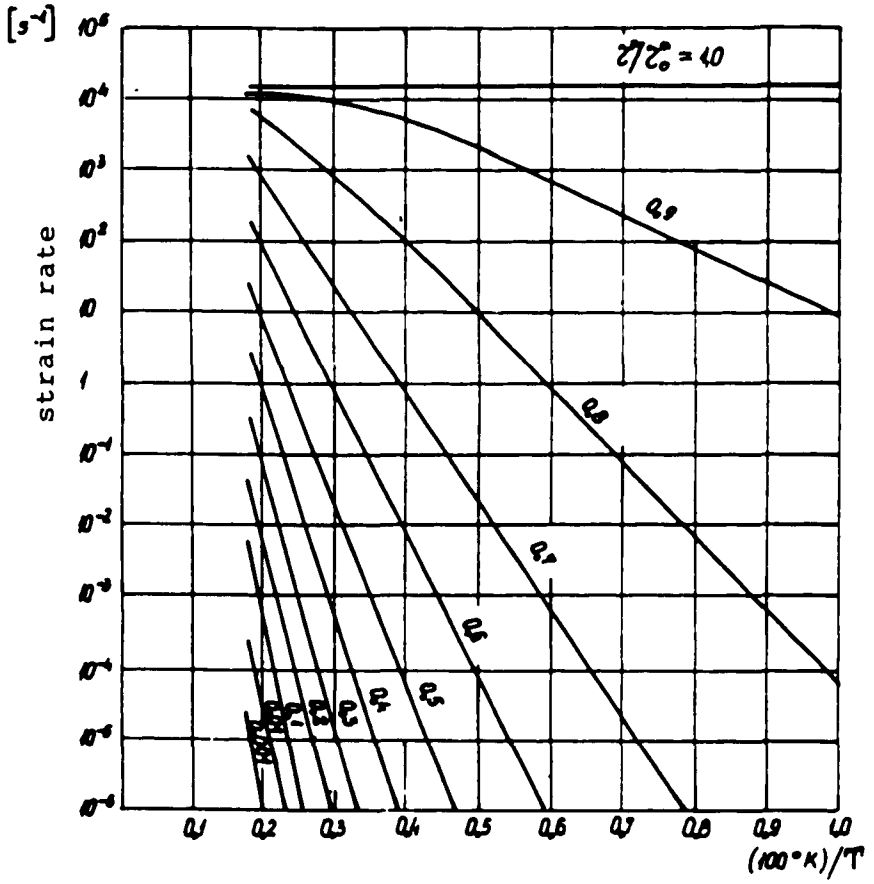


Fig. 7.3. Logarithm of the strain rate versus the inverse of reduced temperature for polycrystalline olivine with grain size 0.1 mm at different stresses.

stress. In this case the glide motion of dislocations is controlled by the number of obstacles. Moreover, the effective stress can be alternatively expressed in the following way:

$$\tau_o^* = \frac{\Delta g}{\Delta V^*} \qquad (7.17)$$

In Fig. 7.1 we show our result for the Log ($t_F/t_w$) versus effective stress for polycrystalline olivine with grain size 0.1 mm at different temperatures. In Fig. 7.2 we review the logarithm of the strain rate versus effective stress for polycrystalline olivine at different temperatures. In Fig. 7.3 we can see the logarithm of the strain rate versus the inverse of reduced temperature for olivine at different stresses. Fig. 7.4 presents the reduced effective stress versus temperature for polycrystalline olivine at different strain rates. Fig. 7.5 shows the yield stress versus temperature for the given strain rate.

The above figures (Fig. 7.1 - 7.5) are our first results in the framework of theormodynamic approach to behavior of olivine from the point of view of dislocations. From these figures we can learn more about obstacles in olivine crystals which dislocations have to overcome and about the temperature dependence in the process of dislocation glide. The yield

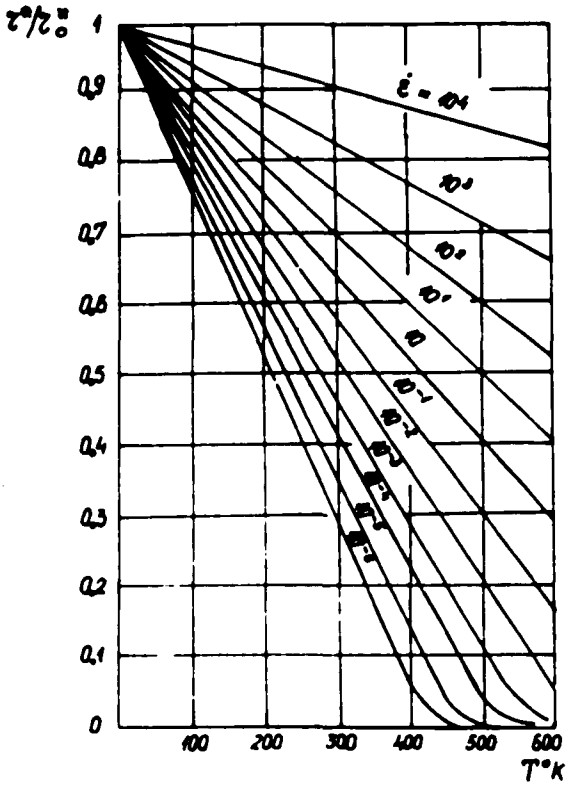


Fig. 7.4. The reduced effective stress versus temperature for polycrystalline olivine with grain size 0.1 mm at different strain rates.

stress versus temperature for the given strain rate for olivine is extremaly important for our consideration on rock fracture in focal zones. The above results are very helpful in our process of optymization because we need some initial values of stresses and strain rates which are the most probable in olivine under subduction conditions.

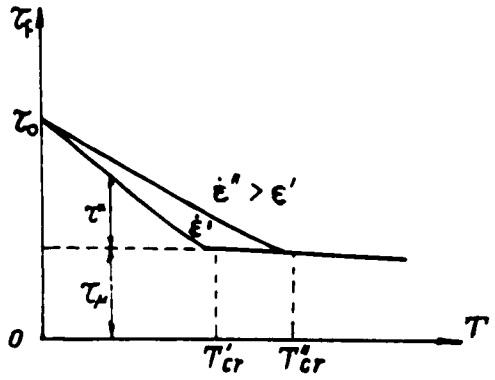


Fig. 7.5. The yield stress versus temperature for the given strain rate.

## 7.1. Numerical identification of material parameters

In this section we shall discuss some aspects of the identification of numerical values of material coefficients contained in constitutive equations describing deformation and fracture. From our experience, we know that direct identification can be applied to simple models, however, a use of computer is necessary when the number of unknown coefficients is greater than 3. In our case the number of unknown parameters for describing the rock material is equal to 5, but the number of unknown parameters describing the Earthquake in our model is equal to 20. In the case of constitutive equations for rocks we have the following 5 parameters: the Young modulus E, the parameter a which is responsible for deformation degradation, the parameter b responsible for stress degradation, and the parameters k and h viscosity in range of plasticity, respectively. An identification of the parameters of the model consists in minimizing the error function. We can estimate the degree of error by measuring the difference between a quantity calculated on the base of theoretical considerations and an analogous quantity obtained from experimental measurements. A mean square deviation is the most frequently applied scalar measure. However, it may lead to some difficulties, if it is applied to a simple difference of variables for very non-linear functions. Two values:

$$Y = \sum_i y_i^2 = \sum_i (f_i^{theor} - f_i^{exper})^2 \qquad (7.18)$$

or

$$X = \sum_i x_i^2 = \sum_i (x_i^{theor} - x_i^{exper})^2 \qquad (7.19)$$

do not give the same result but they ascribe a different weight to different parts of curve. The quadratic mean "distance" avoids these problems and was successfuly applied by Chaboche et al. (1981) (see Fig. 7.6)

$$D = \sum_i d_i^2 = \sum_i \frac{x_i \; y_i}{(x_i^2 + y_i^2)^{\frac{1}{2}}} \qquad (7.20)$$

An advantage of this identification is that we took into account the ordinate Y and abscissa X of error as well. Therefore, the identification of our parameters is very precise here.

If we have assumed a certain error function, then the identification consists in its minimization. In the literature one can find a description of various gradient methods of minimization of error function, particularly the Newton method and its various modifications. It turns out, however, that if one deals with exponential functions, then the gradient methods become divergent what makes their

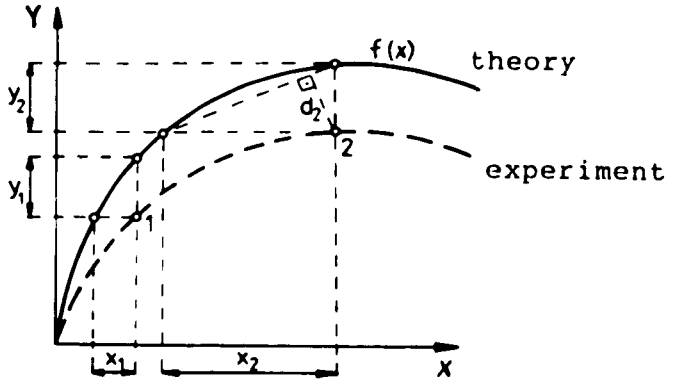


Fig. 7.6. Quadratic mean distance D on a curve. The quantities ($x_1$, $y_1$; $x_2$, $y_2$) are the abscissa and ordinate of error at points 1 and 2, respectively, and $d_2$ is the quadratic mean distance at point 2.

application impossible. Therefore, we applied here the Monte Carlo method, i.e., the method of solving of numerical problems by statistical experiments. At the beginning we assume a certain cube in n-dimensional space, where n equals the number of unknown parameters in our identification which is equal to 5 in the case of constitutive equations for rocks and it is equal to 20 in the case of description of the entire Earthquake process. The corners of this cube correspond to the upper and lower values of our parameters. Next, we find the center of this cube. We treat this point as a starting point of our procedure. At this starting point we calculate a value of error function, which is treated here as an aim function. Next, by using a generator of pseudo-random numbers of normal distribution and another generator of uniform distribution, we randomly establish the direction and size of a step which we shall make from the starting point to the next point. At this new randomly found point we compute a value of aim function. If this new value is less than the value at the former point, then we memorize this smaller value and the coordinates of this point, i.e., the values of our unknown parameters at the point where the aim function obtains the smaller value. In our case, we assumed the number of drawings equals 1000. After computing a value of aim function at 1000 points inside the assumed cube we have found the point where the aim function attained its minimum value. We treated it as a global minimum and as a starting point for another

method, namely the Gauss-Seidl method (stepping method). Around this point we constructed again an n-dimensional cube, but much smaller than previously. Next, inside this cube with an assumed step we were proceeding a systematic search of the set, i.e., at each point we computed a value of aim function. The minimum value found in this way we treated as a local minimum. The identification of rock parameters in our model was carried on the base of experimental results for some rocks. The stress function was treated as an error function. The results of identification are shown in Fig. 7.8 a,b,c,d.

## 7.2. Deformation and stress degradation of rocks

A simple computer model of rock material has been formulated here to investigate a variety of rock behaviors under different strain rates. The most attention was paid to the rock deformation and fracture.

We assume the law of degradation of rock material in the form

$$\dot{\sigma}_o = - a \dot{\epsilon}_v - b \dot{\sigma} - c T \qquad (7.21)$$

This equation can be treated as a criterion of rock fracture. We assumed here that the yield stress $\sigma_o$ is not constant but it decreases with the crack propagation and with the increase of temperature. The parameter a is responsible for a strain degradation, parameter b is responsible for a stress degradation and parameter c is responsible for a thermal degradation. Moreover, we assumed an additive decomposition of the total strain rate into the elastic and inelastic (irreversible or plastic) strain rates

$$\dot{\epsilon} = \dot{\epsilon}_e + \dot{\epsilon}_v \qquad (7.22)$$

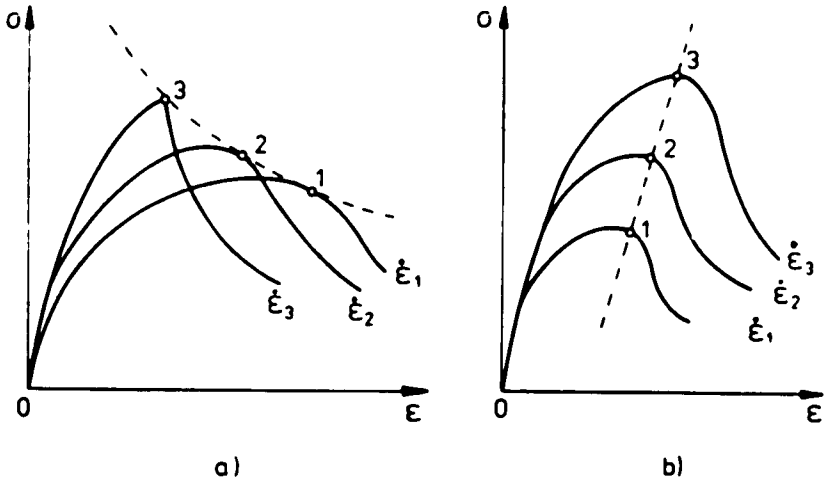


Fig. 7.7. Two types of reactions of rocks for different strain rates.

We use the Hook law for the elastic strain rate

$$\dot{\epsilon}_e = \frac{\dot{\sigma}}{E} \qquad (7.23)$$

and we assume the Bingham model for the inelastic (irreversible) strain rate

$$\dot{\epsilon}_v = \frac{1}{\mu} \langle \sigma - \sigma_o \rangle \qquad (7.24)$$

After same considerations and solving a second-order differential equation we obtain a relationship between the stress $\sigma$ and the strain $\varepsilon$

$$\sigma = -\frac{1+b}{A^2} c \exp\left[\frac{E A}{c} (\epsilon_o - \epsilon)\right] + \frac{a}{A} (\epsilon_o - \epsilon) + \frac{1+b}{A^2} c + \sigma_{oo} \qquad (7.25)$$

and

$$\sigma_o = (1 - A)\ \sigma + a\ (\epsilon_o - \epsilon) + A\ \sigma_{oo} \qquad (7.26)$$

*where* $c = \epsilon\ \mu \quad \Lambda \quad \sigma_{oo} = \sigma_o\ (t = t_o)$ ,

and

$$A = 1 - \frac{a}{E} + b \qquad (7.27)$$

From experimental data presented in Fig. 1.4 and Fig. 1.5 we conclude that there exist two types of reactions of rocks for different strain rates. These two types are shown in Fig. 7.7. In Fig. 7.7 we can see that some rock materials behave in such a way that they strength decreases when the strain rate increases (Fig. 7.7a). Conversely, there are some rock materials which behave in such a way that they strength increases when the strain rate increases as well (Fig. 7.7b). From these figures we can learn about behavior of particular rocks during a straining process.

In Fig. 7.8 a,b we have a comparison of the theoretical compression curves from our model and experimental curves at different strain rates for: a) brittle sandstone with a silty binder, b) lime massive dolomite with a crystal structure. The rocks were tested by Frelkiewicz et al. (1981). Theoretical curves are drawn with a continuous line.

In Fig. 7.8 c,d we can observe a comparison between the theoretical compression curves from our model and experimental curves at different strain rates for: c) compact sandstone with a carbonate binder, d) fine-crystalline streaked dolomite.

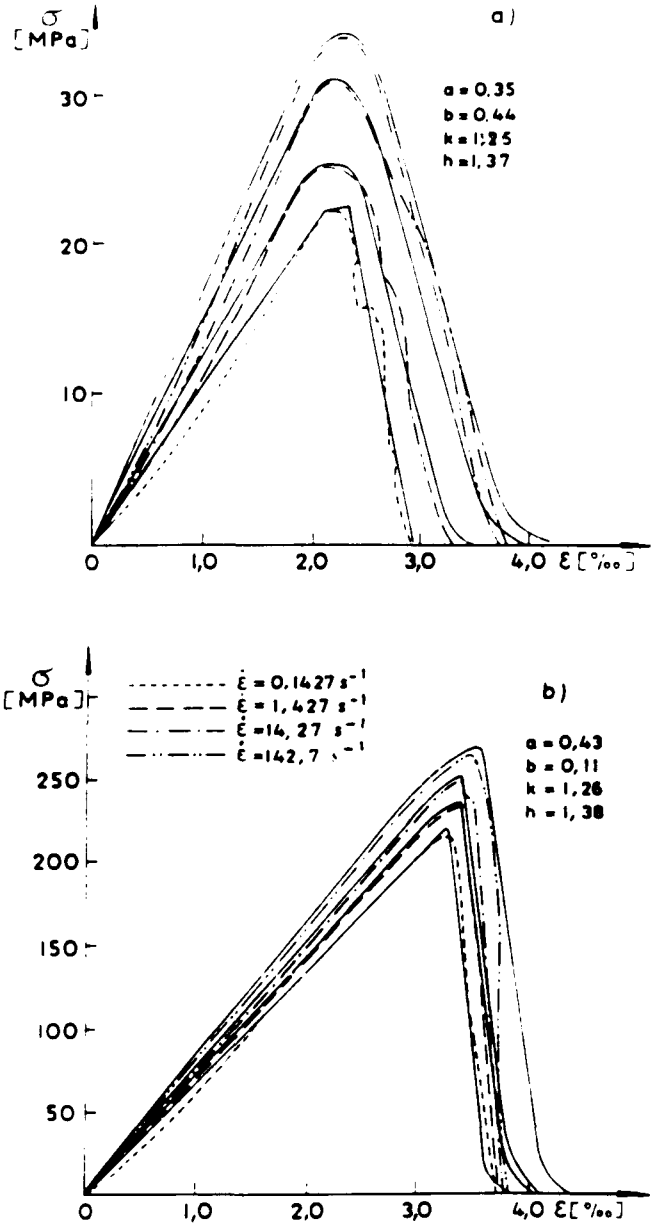


Fig. 7.8. Comparison of the theoretical compression curves from our model and wxperimental curves at different strain rates for: a) brittle sandstone with a silty binder, b) lime massive dolomite with a crystal structure. Rocks tested by Frelkiewicz et al. (1981). Theoretical curves are drawn with a continuous line.

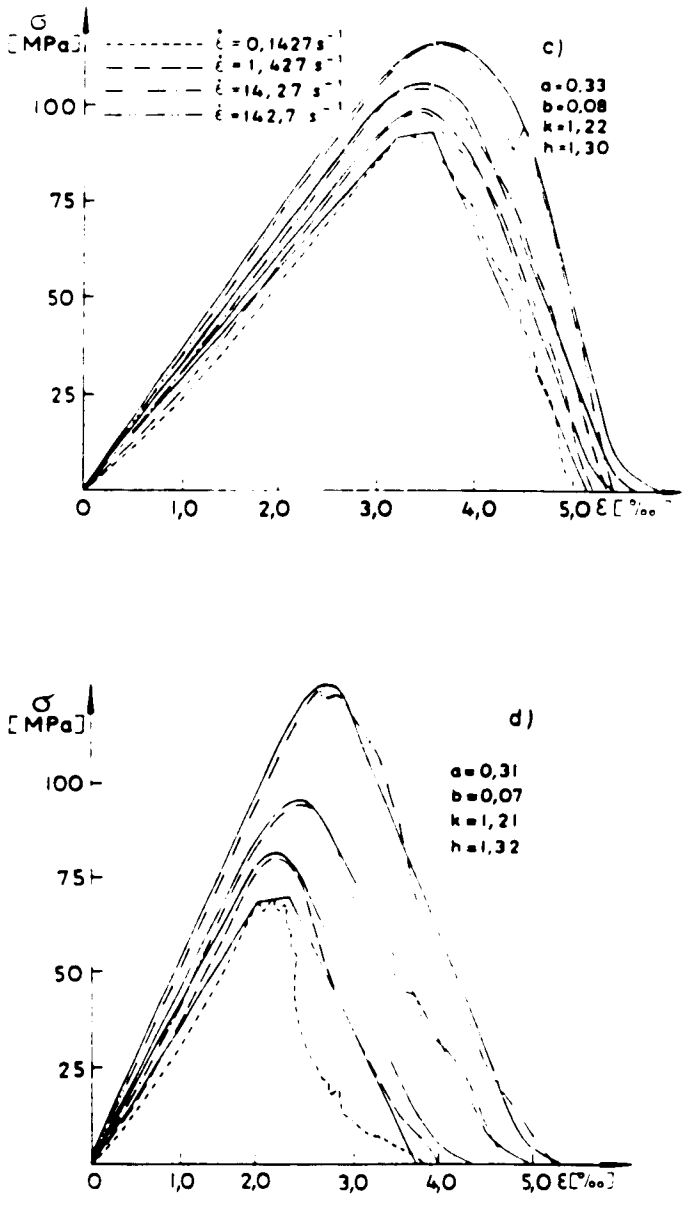


Fig. 7.8. Comparison of the theoretical compression curves from our model and experimental curves at different strain rates: c) compact sandstone with a carbonate binder, d) fine-crystalline streaked dolomite. Rocks tested by Frelkiewicz et al. (1981). Theoretical curves are drawn with c cntinuous line.

All these comparisons between the theoretical compresion curves from our model and experimental curves at different strain rates for some rocks are very helpful in my thesis because I shall use the obtained material parameters: shear modulus, viscosity parameters and different strain rates in the optymization process as initial values of parameters considered. In focal zones we face much higher pressure and higher temperature than presented in the above figures. However, these results are very useful for our optymization procedure because they are very well established and they allow us to start the entire optymization process.

## 8. Numerical identification of Earthquake parameters

Now, we have to apply the aforementioned optimization technique in order to find such a theoretical curve for strain (as a function of time) which has the best possible fit to the curve recorded at a seismic station.

In the process of optimization we have to describe the best values of the following 20 parameters: $C_1$, $C_2$, $C_3$, $C_4$, $d^f$, $d^a$, $d^m$, b, $M_q$, $\Lambda$, C, c, $\kappa$, $\alpha_d$, $\alpha$, L, $v_F$, v, w, $\mu$. From the obtained best values of these parameters we can make some conclusions about the mineralogical composition of a focal region of an Earthquake.

In Fig. 8.1 we compare the theorectical strain as a function of time derived in this study with strains obtained from measurements from 1983 Japan Sea Earthquake showing samples of the strain events. The upper plot shows one event; the lower plot shows five events on a compressed time scale. The one-sided signals have a duration of about three hours. High-frequency variations are due to local noise source, and the long-duration variations (days in duration) result from changes in atmospheric pressure. Tidal frequences have been removed. The smooth line through the data is the calculated variation due to the source modeled by slow slip on an extension of the seismic rupture plane. The solid line denotes our results. Measured data are from a work by

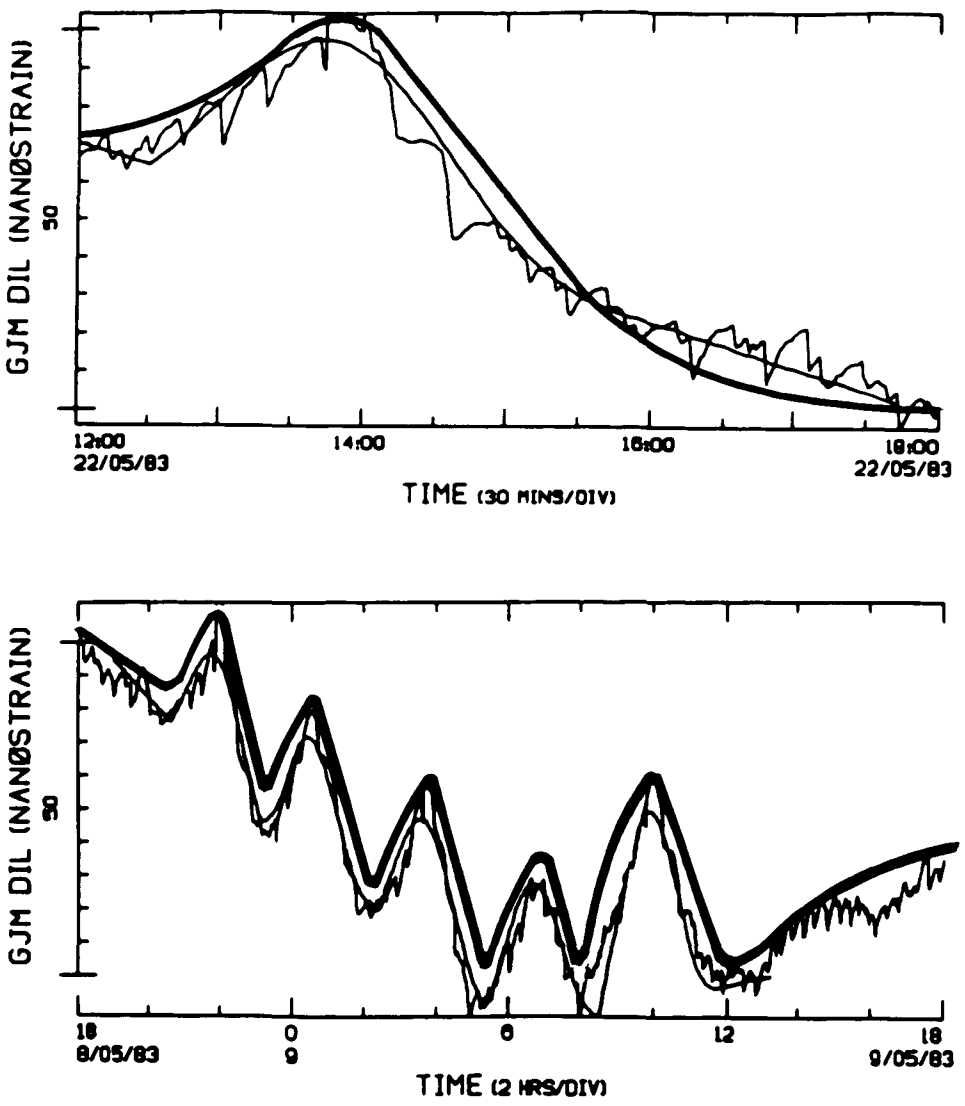


Fig. 8.1. Comparison of the theoretical strain as a function of time derived in this study and data obtained from GJM showing samples of the strain events. Upper plot shows one event; lower plot shows five events on a compressed time scale. The one-sided baylike signals have a duration of about three hours. High-frequency variations are due to a local noise source, and the long-duration variations (days in duration) result from changes in atmospheric pressure. Tidal frequencies have been removed. The smooth line through the data is the calculated variation due to the source modeled by slow slip on an extension of the seismic rupture plane. The solid line denotes our results. (Measurements data from Linde A. and Sacks S., 1989).

Linde and Sacks (1989). The magnitude of this Earthquake is 7.7. The Earthquake took place in 1983 in the Tohoku (northeastern) region of Honshu, Japan. Here GJM denotes the borehole strainmeter site.

From our optimization procedure we came into a conclusion that the best set of parameters describing the focal region of this Earthquake fits to thermodynamical parameters of quartz. Therefore, the focal region of this Earthquake is rich in quartz.

In Fig. 8.2 we review a comparison between the theoretical strain as a function of time derived in this study and obtained from spectra of Earth strain recorded at Isabella, California, for the 1960 Chilean and 1964 Alaskan Earthquakes. Here $\delta$ is the angle between the strain seismometer axis and the great circle path to the epicenter. Observational data are from a paper by Smith (1967). Theoretical results are denoted by the solid line.

From our optimization procedure applied to the 1960 Chilean Earthquake we have obtained a set of parameters which has the best fit with olivine as the rock material. Therefore, we conclude that the focal region of the 1960 Chilean Earthquake was in a zone comprised mainly of olivine. The same conclusion was drawn about the 1964 Alaskan Earthquake. We

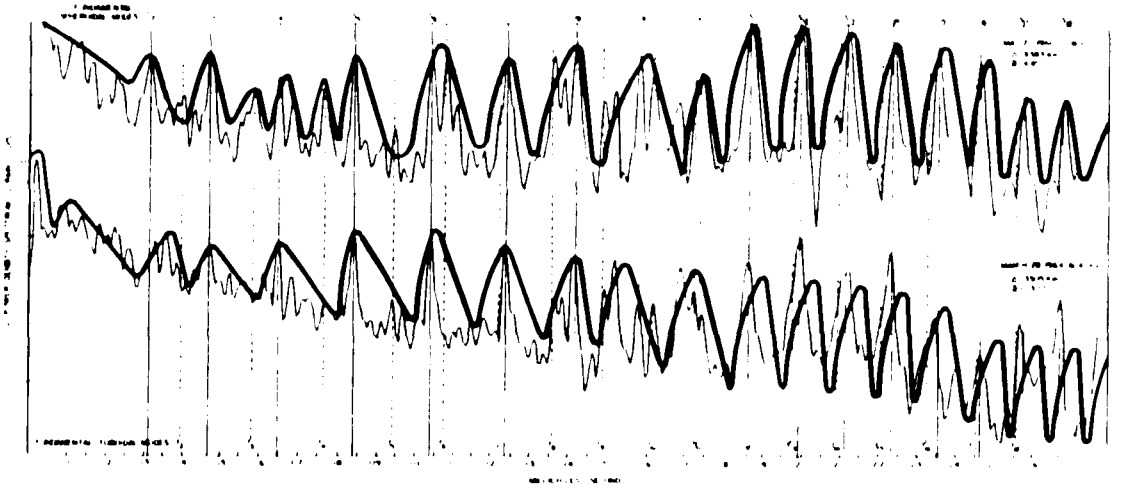

Fig. 8.2. Comparison of the theoretical strain as a function of time derived in this study and obtained from measurements spectra of Earth strain recorded at Isabella, California, for the 1960 Chilean and 1964 Alaskan Earthquakes, $\delta$ is the angle between the strain seismometer axis and the great circle path to the epicenter. Data from Smith (1967). Theoretical results are denoted by the solid line.

should emphasize a good agreement between the theoretical curves and those obtained from measurements.

## 9. THE SEISMIC MOMENT

From the thermodynamic considerations it follows that a body containing some number of dislocations cannot be in a state of equilibrium; there is no minimum of the Gibbs function because by reducing the number of dislocations we get always smaller value of the free energy. For a dense distribution of dislocations we can assume, however, that there exists a certain superlattice composed with dislocations which interact between themselves. We refer here, of course, to a kind of random distribution of dislocations: taking a mean value of distance or using a notion of dislocation density ($nb/\Delta S$, b - the Burgers displacement vector, n - a number of dislocations crossing a surface element $\Delta S$) we may introduce a regular superlattice with a characteristic distance $\Lambda$ ($\Lambda^2 = \Delta S/n$).

By analogy with the thermodynamics of the point defects we can find an equilibrium value which is related to the line vacancies that are in a real material when comparing it with a material with regular superlattice.
It is given by the following formula

$$m_{eq} = M \exp\left(-\frac{g}{kT}\right) , \quad \forall \quad \alpha = \frac{b}{\Lambda^2} \exp\left(-\frac{g}{kT}\right) \qquad (9.4)$$

where $m_{eq}$ is an equilibrium number of line vacancies; 3M is a number of dislocations in a body (M is a number of

dislocations per surface); $\vartheta$ is a formation energy for a line vacancy ( that contributes to the Gibbs energy function); $\kappa$ is the Boltzmann constant.

For a regular superlattice with constant $\Lambda$ a density of dislocations is evidently given by $\alpha^{\circ} = b/\Lambda^2$. Hence an equilibrium density of dislocations becomes

$$\alpha_{eq} = \alpha^{\circ} - \hat{\alpha} = \frac{b}{\Lambda^2}\left[1 - \exp\left(-\frac{\vartheta}{\kappa T}\right)\right] \qquad (9.5)$$

and a drop of density may be put as:

$$\Delta\alpha = \alpha^{\circ} - \alpha_{eq} = \hat{\alpha} \qquad (9.6)$$

This equilibrium density may be useful for us when looking for the most probable density value of defects after an energy release in a fracturing process.
A seismic moment equals

$$M = \mu\, b\, \Delta S = \mu\, b\, \Lambda^2\, M \qquad (9.7)$$

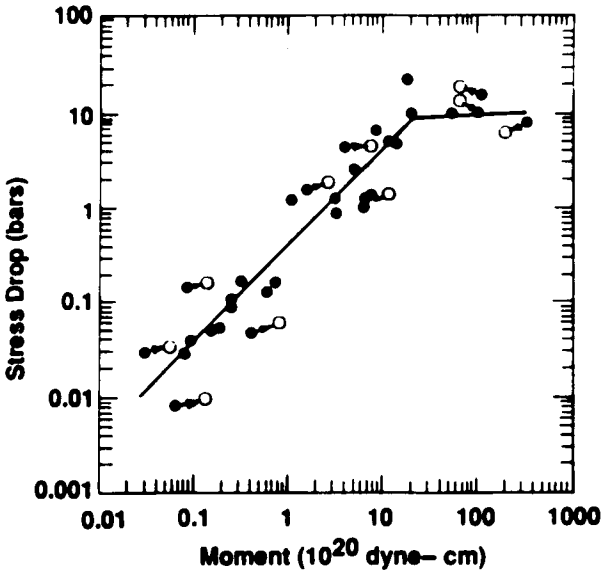


Fig. 9.1. Comparison of the seismic moments obtained in this study and seismic moments from measurements. The diagram shows the stress drop during an earthquake versus seismic moment which is a measure of magnitude.
o - theoretical results from our model,
● - results from measurements (Linde and Sacks, 1989).
The corresponding pairs of events are connected by arrows.

We can express it by an equilibrium value $m_{eq}$ (6.4) which corresponds to a value of a density drop (comp. (6.6) and (6.4)):

$$M = M^{o}\, m \exp\left(\frac{\vartheta^{f}}{\kappa T}\right) \qquad (9.8)$$

where $M^{o} = \mu\, b\, \Lambda^{2}$ is an elementary value of seismic moment for a given structure. Using (6.5) we can write a seismic moment for a given energy release

$$M = M^{o}\, \Delta E\, \frac{\exp\left(\frac{\vartheta^{f}}{\kappa T}\right)}{\kappa T} \qquad (9.9)$$

This formula gives an important relation between an energy release and a seismic moment e.g., for a given $\Delta E$ a seismic moment decreases with temperature.

Fig. 9.1 shows a comparison of the seismic moments obtained in this study and seismic moments from measurements. The diagram shows the stress drop during an Earthquake versus seismic moment which is a measure of magnitude. The theoretical results and corresponding results from measurements are connected by arrows. We can observe a very good agreement of our results with those oberved by Linde and Sacks (1989).
In Fig. 9.2 we also have a comparison of the seismic moments

obtained in this study and seismic moments from measurements. In this case, however, the diagram shows the fault length (radius) versus seismic moment. Here we can see an excellent agreement between our theoretical results and the results from measurements (measurement data from Linde and Sacks, 1989).

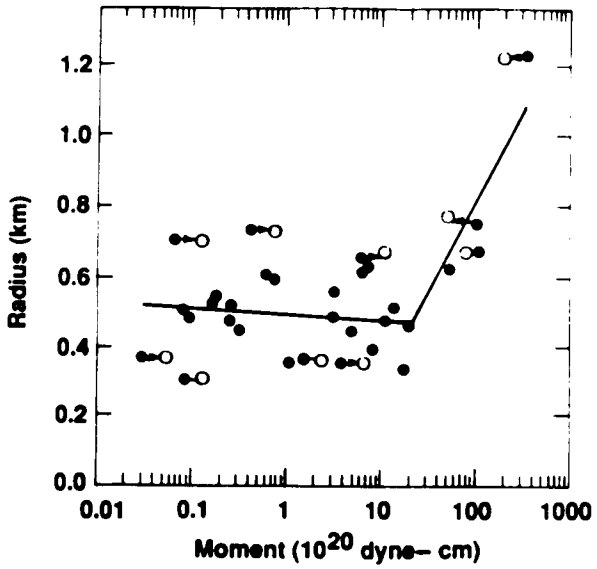


Fig. 9.2. Comparison of the seismic moments obtained in this study and seismic moments from measurements. The diagram shows the fault length (radius) versus seismic moment which is a measure of magnitude.
o - theoretical results from our model,
● - results from measurements (Linde and Sacks, 1989).
The corresponding pairs of events are connected by arrows.

## 10. THE ENTROPY JUMP DURING AN EARTHQUAKE

Now, a formation energy of line vacancy can be written down as follows

$$g^f = \tau\, b\, \Lambda^2$$

We have for entropy

$$(\textit{neglecting } \hat{S}^f = -\frac{\partial g^f}{\partial T}\Big|_\tau = 0)$$

$$S = S^o + m\kappa\,(1 + \frac{g^f}{\kappa\, T}) = S^o + m\,\kappa\,(1 + \frac{\tau\, b\, \Lambda^2}{\kappa\, T})$$

hence

$$\delta S = \kappa\, \delta m + \frac{m\, b\, \tau}{T}\, 2\, \Lambda\, \delta\Lambda = \kappa\, \delta m - \frac{m\, \tau\, b}{T}\, \frac{\Lambda^2}{M}\, \delta M$$

(because

$$\frac{\Delta S}{M} = \Lambda^2 \quad , \quad \Delta S \text{ - surface element,}$$

$$\textit{hence } \delta M = -\frac{2M\, \delta\Lambda}{\Lambda})$$

For premonitory processes we have:

$$\delta S = \delta S_i + \delta S_e \geq 0$$

Inside the system: we can assume that a number of dislocations increases $\delta M > 0$ and a number of vacancies decreases $\delta m < 0$

$$\delta S_i = \kappa \delta m - \frac{m \tau b}{T} \frac{\Lambda^2}{M} \delta M < 0$$

Outside the system: we have conversely $\delta m > 0$, $\delta M < 0$.

$$\delta S_e > 0$$

For rebound processes (including earthquake events) we can assume that the number of dislocations rapidly decreases (due to processes of dislocation pair annihilation).
Hence, we have $\Delta M < 0$ and thus

$$\delta S_i = -\frac{m \tau b}{T} \frac{\Lambda^2}{M} \Delta M > 0 \quad .$$

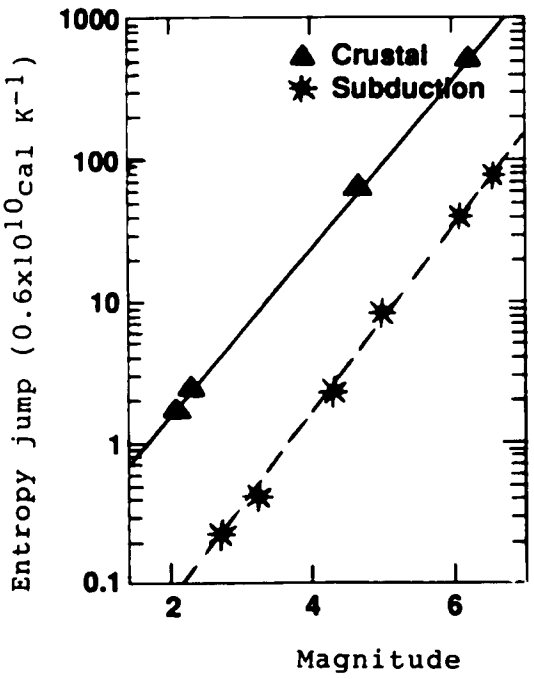


Fig. 10.1. The entropy jump during an earthquake versus the magnitude.

We have proven by the above relation that we deal with a jump increase of entropy during an earthquake process.

In Fig. 10.1 we show the entropy jump during an Earthquake versus the magnitude. We can observe two groups of Earthquakes: shallow crustal and deep Earthquakes (in subduction zones). Separately in both groups there is a proportional relationship between the entropy jump and the magnitude. Generally speaking, the Earthquakes in subduction zones have smaller entropy than crustal Earthquakes. From this figure we can conclude that the entropy jump during an Earthquake is as good a measure of an Earthquake as the magnitude.

## 11. CONCLUSIONS

A completely new thermodynamics of line defects has been formulated in this paper. We assumed a very important linear relationship between the defect formation Gibbs free energy and the shear bulk modulus.

Starting from thermodynamics of line defects we have obtained some relationships for the waiting time of dislocation, effective stresses, and strain rates in olivine.
Due to the fact that from our very precise description of the rocks on a microscopic level we have a remarkable number of thermodynamic parameters (i.e., 20 parameters) and their identification for an earthquake process gives a lot of information about the investigated seismologically active regions of the Earth, we have obtained some information concerning the most probable mineralogical composition of the rocks forming the considered Earthquake zone. Namely, we came to the conclusion that the focal zone of the 1983 Japan Sea Earthquake in Tohoku (northeastern) region of Honshu, Japan is a material rich in quartz. We should emphasize the excellent agreement between our theoretical curves with those observed by Linde and Sacks (1989).

Moreover, our computation of the 1960 Chilean and 1964 Alaskan Earthquakes have given a result that the focal zones of these

Earthquakes are a material rich in olivine. In this case there is also a very good agreement between our theoretical curves with those observed by Smith (1967).

In addition, we compute seismic moments and compare them with measurements obtained by Linde and Sacks (1989).
The entropy jump during an earthquake was also computed. The entropy jump is as good in describing an Earthquake as its seismic moment.

Many authors express the opinion that shallow Earthqukes are produced by brittle shear fracture of rock and frictional sliding on pre-existing fault surfaces (cf. Scholz, 1990; Green et al., 1990; Kirby et al., 1991). They regard that in the case of deep Earthquakes in subduction zones, i.e., at very high pressures brittle fracture and frictional sliding are impossible because frictional resistance to movement on any potential fault surface is so great that ductile stress-relief processes accomodate strain at lower shear stresses than those necessary to activate faulting. Nevertheless, according to Green et al. (1990), more than 20% of Earthquakes with magnitude greater than five occur at depth greater than 300 km, where the pressure exceeds 10 GPa. Possible explanations for this paradox have been offered by several recent experimental studies of shearing instabilities associated with phase transformations at high pressure. One

of these mechanisms is associated with anticrack development during the olivine - spinel ( $\alpha \rightarrow \gamma$ ) phase transformation in $Mg_2GeO_4$ at pressures of 1 - 2 GPa. We should emphasize that it is particualarly attractive because it operates between mineral structures known to occur in the mantle. Green et al. (1990) showed that this mechanism also can operate in natural silicate olivine, $(Mg, Fe)_2 SiO_4$, during onset of the $\alpha \rightarrow \beta$ transformation at the much higher pressures at which deep Earthquakes occur. These results lend strong support to the hypothesis proposed by Green et al. (1990) that the anticrack mechanism is responsible for such Earthquakes.

In my opinion, both factors rock defects and phase transformations are responsible for Earthquakes in subduction zones.

REFERENCES

Bieniawski Z. T., 1970, "Time-dependent behaviour of fractured rock." Rock Mech., 2, 17-26.

Bridgman P.W., 1943, The Nature of Thermodynamics, Harvard University Press, Cambridge, Mass.

Chaboche J. L., Lemaitre J., Marquis D., Savalle S., 1981, "Discussion on problems of models identification", Proc. IUTAM Symposium, Physical Non-linearities in Structure Analysis, Senslis (France) 1980, J. Hult and J. Lemaitre (eds), Springer-Verlag, Berlin.

Dziewonski A. M. and Anderson D. L., 1981, "Preliminary reference Earth model." Phys. Earth Plan. Int., 25, 297-356.

Dziewonski A. M., Hales A. L. and Lapwood E.R., 1975, "Parametrically simple models consistent with geophysical data.", Phys. Earth Plan. Int., 10, 12-48.

Frelkiewicz S., Kijewski P. and Lis J., 1981," Model of testing of real materials for specification of rock burst mechanisms." CUPRUM, Wroclaw (in Polish).

Gibbs J.W., 1906, "On the equilibrium of heterogeneous substances.", in: The Scientific Papers of J. Willard Gibbs, vol. 1, Longmans, Green and Comp., Toronto, 55-349.

Glansdorff G. and Prigogine I., 1971, Thermodynamics of Irreversible Processes. J. Wiley, New York.

Green II H.W., Young T.E., Walker D. and Scholz C.H., 1990, "Anticrack-associated faulting at very high pressure in natural olivine.", Nature, V. 348, No. 6303, pp. 720-722.

Hull D., 1975, Introduction to Dislocations, 2nd edn., Pergamon Press, Oxford.

Kirby S.H., Durham W.B and Stern L.A., 1991, "Mantle phase changes and deep-earthquake faulting in subduction lithosphere", Science, 252, 216-225.

Kocks U. F., Argon A. S. and Ashby M.F., 1975, Thermodynamics and Kinetics of Slip., Pergamon Press, Oxford, New York.

Linde A. and Sacks S., 1989, "Earthquakes and crustal deformation." in: Year Book 89, The President's

Report, Carnegie Institution of Washington, D.C.

Majewski E., 1984, "A postulate of inelasticity in finite viscoplasticity.", in: Advances in Rheology, Proc. IX Intern. Congress on Rheology, Vol. 4, Applications, B. Mena et al. (eds.), Acapulco, Mexico, October 8-13, Elsevier Sci. Publ. Comp., Amsterdam - New York.

Majewski E., 1985a, "Nonequilibrium thermodynamics of the processes at the core-mantle boundary in the Earth's interior.", Programme Supplement, EUG III, 1-4 April 1985, Strasbourg, France, p. 14.

Majewski E., 1985b, "Nonequilibrium thermodynamics of melting and solidification processes at the inner-outer core boundary in the Earth's interior.", Acta Geophys. Polonica, 33, No. 4, 429-437.

Majewski E., 1986a, "Nonequilibrium thermodynamics of the core-mantle boundary in the Earth's interior.", Book of Abstracts, paper 6.7, The 9-th IUPAC Conference on Chemical Thermodynamics, July 14-18, 1986, Lisboa, Portugal, Callouste Gulbenkian Foundation.

Majewski E., 1986b, "Thermodynamics of the inner-outer core boundary in the Earth's interior.", Book of Abstracts,

Joint Meeting of the European Geophysical Society and the European Seismological Commission, August 21-30, 1986, Kiel, West Germany.

Majewski E., 1986c, "Initiation of rock fracture at different rates. An attempt of modelling of the mining tremor processes based on dynamic plasticity.", Publs. Inst. Geophys. Pol. Acad. Sc., M-8 (191), 11-38 , Polish Scientific Publishers, Warsaw, Lodz (in Polish).

Majewski E., 1987, "Nonequilibrium thermodynamics of processes at the inner-outer core boundary in the Venus' interior.", in: Lunar and Planetary Science XVIII, Lunar and Planetary Institute, Houston, USA.

Majewski E., 1988, Theory of Large Dynamic Deformations of Rock Body., Publs. Inst. Geophys. Pol. Acad. Sc., M-9 (201), pp. 218, Polish Scientific Publishers, Warsaw, Lodz (in Polish).

Majewski E., 1989, "Molodensky boundary-value problem.", in: Gravity and Low-Frequency Geodynamics, R. Teisseyre (ed.), vol. 4 of series: Physics and Evolution of the Earth's Interior, R. Teisseyre (ser. ed.), Elsevier Sci. Publ. Comp., Amsterdam-New York.

Majewski E., 1991a, "Thermodynamical approach to evolution.", in: Dynamics of the Earth Evolution., L. Czechowski, R. Teisseyre and J. Leliwa-Kopystynski (eds.), vol. 6 of series: Physics and Evolution of the Earth's Interior, R. Teisseyre (ser. ed.), Elsevier Sci. Publ. Comp., Amsterdam - New York (in press).

Majewski E., 1991b, "The convection stability in an anisotropic Earth's mantle", Acta Geophysica Polonica (in press).

Majewski E., 1991c, "The finite-amplitude convection in an anisotropic Earth's mantle.", Acta Geophysica Polonica (in press).

Mroz Z. and Majewski E., 1989, "Dynamic model of damage of coal and of some rocks for specification of rock burst mechanisms.", Archives of Mining Sciences, Vol.34, Issue 1, p. 65-95, (in Polish).

Peng S.S. and Podniesk E.R., 1972, "Relaxation and the behaviour of failed rock". Int. J. Rock Mech. Min. Sci., 9.

Prigogine I., 1969, Thermodynamics of Irreversible

Processes., John Wiley and Sons Inc., New York.

Prigogine I., 1978, Thermodynamics of Irreversible Processes, 3rd edition, John Wiley and Sons Inc., New York.

Ranalli G., 1987, Rheology of the Earth. Deformation and Flow Processes in Geophysics and Geodynamics., Allen & Unwin, Boston, London, Sydney, Wellington.

Saxena S.K., 1973, Thermodynamics of Rock-Forming Crystalline Solutions, Springer-Verlag, New York.

Scholz C.C.H., 1990, The Mechanics of Earthqukes and Faulting, Cambridge University Press, Cambridge.

Smith S.W., 1967, "Free vibrations of the Earth", in: International Dictionary of Geophysics, Runcorn S.K. et al. (eds), Pergamon Press, Oxford, p. 344.

Suppe J., 1989, Principles of Rock Deformations and Faulting, Academic Press, New York.

Teisseyre R., 1980, "Earthquake premonitory sequence-dislocation processes and fracturing.", Boll. Geofis. Teor. Appl., XXII: 245-254.

Teisseyre R., 1985a, "New earthquake rebound theory.", Phys. Earth Planet. Int., 39, 1-4.

Teisseyre R., 1985b, "Creep flow and earthquake rebound: system of internal stress evolution. Acta Geophys. Pol., XXXIII, 1

Teisseyre R., 1987, "Earthquake generation in different stress states.", Phys. Earth Planet. Int., 49, 24-29.

Toksoz M.N., 1982, "The subduction of the lithosphere." in: Volcanoes and the Earth's Interior, Scientific American, Freeman, 6-16.

Vassiliou M.S., Hager B.H. and Raefsky A., 1984, "The distribution of Earthquakes with depth in stress in subducting slabs.", J. Geodynam., 1, 11-28.

Varotsos P.A. and Alexopoulos K.D., 1986, Thermodynamics of Point Defects and Their Relation with Bulk Properties., North - Holland, Amsterdam, New York.